

Synthesis, molecular modeling and SAR study of novel pyrazolo[5,1-f][1,6]naphthyridines as CB2 receptor antagonists/inverse agonists

Questa è la versione Post print del seguente articolo:

*Original*

Synthesis, molecular modeling and SAR study of novel pyrazolo[5,1-f][1,6]naphthyridines as CB2 receptor antagonists/inverse agonists / Dore, A.; Asproni, Battistina; Scampuddu, A.; Gessi, S.; Murineddu, Gabriele; Cichero, E.; Fossa, P.; Merighi, S.; Bencivenni, S.; Pinna, Gerard Aime. - In: BIOORGANIC & MEDICINAL CHEMISTRY. - ISSN 0968-0896. - 24:21(2016), pp. 5291-5301. [10.1016/j.bmc.2016.08.055]

*Availability:*

This version is available at: 11388/174182 since: 2022-05-27T11:29:31Z

*Publisher:*

*Published*

DOI:10.1016/j.bmc.2016.08.055

*Terms of use:*

Chiunque può accedere liberamente al full text dei lavori resi disponibili come "Open Access".

*Publisher copyright*

note finali coverpage

(Article begins on next page)

**Synthesis, molecular modeling and SAR study of novel pyrazolo[5,1-f][1,6]naphthyridines as  
CB<sub>2</sub> receptor antagonists/inverse agonists**

Antonio Dore<sup>a</sup>, Battistina Asproni<sup>a\*</sup>, Alessia Scampuddu<sup>a</sup>, Stefania Gessi<sup>b\*</sup>, Gabriele Murineddu<sup>a</sup>, Elena Cichero<sup>c</sup>, Paola Fossa<sup>c</sup>, Stefania Merighi<sup>b</sup>, Serena Bencivenni<sup>b</sup>, Gérard A. Pinna<sup>a</sup>.

<sup>a</sup>*Dipartimento di Chimica e Farmacia, Università degli Studi di Sassari, Via F. Muroli 23/a, 07100 Sassari, Italy*

<sup>b</sup>*Dipartimento di Scienze Mediche, Sezione di Farmacologia, Università di Ferrara, Via Fossato di Mortara, 17-19, 44121 Ferrara, Italy*

<sup>c</sup>*Dipartimento di Farmacia, Università di Genova, Viale Benedetto XV n. 3, 16132, Genova, Italy*

Corresponding authors:

**B. Asproni**

Dipartimento di Chimica e Farmacia, Università degli Studi di Sassari, Via F. Muroli 23/a, 07100 Sassari, Italy

Tel: +39 079 228749; e-mail: asproni@uniss.it

**S. Gessi**

Dipartimento di Scienze Mediche, Sezione di Farmacologia, Università di Ferrara, Via Fossato di Mortara, 17-19, 44121 Ferrara, Italy

Tel: +39 0532 455332; e-mail: gss@unife.it

## Abstract

Pyrazolo[5,1-*f*][1,6]naphthyridine-carboxamide derivatives were synthesized and evaluated for the affinity at CB<sub>1</sub> and CB<sub>2</sub> receptors. Based on the AgOTf and proline-cocatalyzed multicomponent methodology, the ethyl 5-(*p*-tolyl)pyrazolo[5,1-*f*][1,6]naphthyridine-2-carboxylate (**12**) and ethyl 5-(2,4-dichlorophenyl)pyrazolo[5,1-*f*][1,6]naphthyridine-2-carboxylate (**13**) intermediates were synthesized from the appropriate *o*-alkynylaldehydes, *p*-toluenesulfonyl hydrazide and ethyl pyruvate. Most of the novel compounds feature a *p*-tolyl (**8a-i**) or a 2,4-dichlorophenyl (**8j**) motif at the C<sub>5</sub>-position of the tricyclic pyrazolo[5,1-*f*][1,6]naphthyridine scaffold. Structural variation on the carboxamide moiety at the C<sub>2</sub>-position include basic monocyclic, terpenoid and adamantane-based amines. Among these derivatives, compound **8h** (*N*-adamant-1-yl-5-(*p*-tolyl)pyrazolo[5,1-*f*][1,6]naphthyridine-2-carboxamide) exhibited the highest CB<sub>2</sub> receptor affinity ( $K_i = 33$  nM) and a high degree of selectivity ( $K_i\text{CB}_1/K_i\text{CB}_2 = 173:1$ ), whereas a similar trend in the near nM range was seen for the bornyl analogue (compound **8f**,  $K_i = 53$  nM) and the myrtanyl derivative **8j** ( $K_i = 67$  nM). Effects of **8h**, **8f** and **8j** on forskolin-stimulated cAMP levels were determined, showing antagonist/inverse agonist properties for such compounds. Docking studies conducted for these derivatives and the reference antagonist/inverse agonist compound **4** (SR144528) disclosed the specific pattern of interactions probably related to the pyrazolo[5,1-*f*][1,6]naphthyridine scaffold as CB<sub>2</sub> inverse agonists.

**Keywords:** Pyrazolo[5,1-*f*][1,6]naphthyridine; Cannabinoid receptors; CB<sub>2</sub> antagonism/inverse agonism; Docking studies

## 1. Introduction

The endocannabinoid system indicates a whole signalling system that comprises cannabinoid receptors, endogenous ligands exemplified by *N*-arachidonylethanolamine (AEA, anandamide) **1** and 2-arachidonoylglycerol (2-AG) **2** (Fig. 1) and enzymes for ligand biosynthesis and inactivation.<sup>1,2</sup> This signalling system plays a crucial role in numerous physiological and pathological functions and it is involved in maintaining the physiological steady state and homeostasis.<sup>3</sup>

There are two subtypes of cannabinoid receptors discovered so far, the cannabinoid type 1 receptor (CB<sub>1</sub>R) and the cannabinoid type 2 receptor (CB<sub>2</sub>R),<sup>4</sup> which belong to the rhodopsin-like family of G-protein-coupled receptors (GPCRs).<sup>5</sup> Even before the endogenous ligands were known, CBRs have been described to be activated by terpenoid plant constituents, e.g., by  $\Delta^9$ -tetrahydrocannabinol ( $\Delta^9$ -THC) **3**, the major psychoactive component of *Cannabis sativa*.<sup>6</sup>

<<Insert Figure 1>>

The CB<sub>1</sub>Rs are abundantly expressed in the central nervous system (CNS) and are responsible for the psychotropic effects observed with nonselective cannabinoid ligands.<sup>7-10</sup> The CB<sub>2</sub>Rs were initially identified as a peripherally restricted receptors predominantly expressed in cells of the human immune system,<sup>11-13</sup> and therefore playing an important role in mediating the immune-modulatory function.<sup>14</sup> Subsequent data, however, have also demonstrated the presence of CB<sub>2</sub>Rs in brain, albeit to a much lesser extent,<sup>15</sup> myocardium, cardiomyoblasts and endothelial cells of various origins.<sup>16</sup>

Recent studies have demonstrated that CB<sub>2</sub>Rs are involved in numerous diseases.<sup>17</sup> Several selective CB<sub>2</sub>R agonists exhibited analgesic activity in preclinical models of acute, inflammatory and neuropathic pain.<sup>18-21</sup> Furthermore, CB<sub>2</sub>R agonists have been evaluated for efficacy in ameliorating disease progression in *in vivo* models of multiple sclerosis,<sup>22</sup> Alzheimer's disease,<sup>23</sup> as well as amyotrophic lateral sclerosis.<sup>24</sup> Recent findings highlight the emerging interest in the development of CB<sub>2</sub>R inverse agonists effective for the control of immune cell mobility in arthritis and autoimmune encephalomyelitis<sup>25</sup> and for the treatment of osteoporosis via the inhibition of osteoclast differentiation.<sup>26</sup> CB<sub>2</sub>R neutral antagonist ligands have been recently described.<sup>27</sup> Such compounds could be useful to ascertain more in detail the role of CB<sub>2</sub> receptor in physiopathological conditions.

Because of the therapeutic potential of CB<sub>2</sub> ligands, there has been an increasing interest in identifying a huge diversity of chemical scaffolds for CB<sub>2</sub> interaction. Within this frame, hundreds of bioactive CB<sub>2</sub>R ligands have been discovered<sup>17,18</sup> and among them, pyrazole derivatives **4** (SR144528)<sup>28</sup> and **5**<sup>29</sup> emerged as important prototypical CB<sub>2</sub> selective ligands (Fig. 2). Compound **4** from Sanofi was identified as the first potent and selective antagonist/inverse agonist of the CB<sub>2</sub>R.

Molecular modeling studies carried out on **4**<sup>30</sup> highlighted the importance of the C<sub>3</sub> carboxamide moiety together with N<sub>1</sub>-methylbenzyl and C<sub>5</sub>-chloromethylphenyl substituents for CB<sub>2</sub>R affinity. A fenchyl group as carboxamide substituent is important for productive CB<sub>2</sub>R interaction. Pyrazole derivative **5** from our lab is a dihydroindenopyrazol-based compound and belongs to one of the first tricycles to be described for CBR affinity. Structure activity-relationship (SAR) studies performed on compound **5** revealed that the flattening of the plane of the tricyclic core was a determining factor in its very high CB<sub>2</sub>-affinity, exceptional selectivity over CB<sub>1</sub>R, and CB<sub>2</sub> agonist activity *in vitro*. Tricyclic derivatives **6**<sup>31</sup> and **7**<sup>32</sup> feature respectively a dihydrothienocyclopentapyrazole and benzofuopyrazole scaffolds. Interestingly, both compounds keep the affinity for CB<sub>2</sub>R in the nM range and are endowed with a good selectivity over CB<sub>1</sub>R, even if lower than that elicited by compound **4** and **5**.

<<Insert Figure 2>>

Pursuing our interest in expanding SAR studies on CB<sub>2</sub>R, we thought that the planar pyrazolo[5,1-*f*][1,6]naphthyridine **8** (Fig. 3) could be an attractive scaffold for designing novel CB<sub>2</sub> ligands. Looking at the structure of compounds **4-7**, we postulated that the introduction of the carboxamide moiety and the pendant N<sub>1</sub>-benzyl substituent into the tricyclic core **8** might provide novel potential CB<sub>2</sub> agonist, antagonist, inverse agonist ligands with potential therapeutic value. Thus novel compounds that varied the carboxamide moiety and the phenyl substitution were designed (Fig. 3 and Tab. 1). In this paper we report the synthesis of compounds **8a-k** together with preliminary aspects of their receptor affinity, selectivity, biological activities and molecular modeling studies. These data are accompanied by a thorough *in silico* evaluation of the pharmacokinetic and toxicity properties of the most potent derivatives here disclosed, with the aim at gaining preliminary information concerning their potentially drug-like profile.

<<Insert Figure 3>>

## 2. Chemistry

The synthetic route to the title compounds **8a-k** is outlined in Scheme 1. Based on the AgOTf and proline-cocatalyzed multicomponent methodology,<sup>33</sup> the key intermediates ethyl 5-(*p*-tolyl)pyrazolo[5,1-*f*][1,6]naphthyridine-2-carboxylate (**12**) and ethyl 5-(2,4-dichlorophenyl)pyrazolo[5,1-*f*][1,6]naphthyridine-2-carboxylate (**13**) were synthesized from the appropriate *o*-alkynylaldehydes, *p*-toluenesulfonyl hydrazide (PTSH) and ethyl pyruvate.

Thus, 2-bromonicotinaldehyde **9** was allowed to react with appropriate alkynes under the

conventional Sonogashira conditions to give the corresponding *o*-alkynylaldehydes **10,11** in good yields. Compounds **10,11** were condensed *in situ* with PTSH in the presence of AgOTf (10 mol %), DL-proline (10 mol %), to give the corresponding hydrazones **10',11'** (not isolated), which were converted into the desired tricyclic pyrazoles **12,13** by sequential treatment with ethyl pyruvate, heating the reaction mixture by microwave irradiation to 50-60 °C, and with Na<sub>2</sub>CO<sub>3</sub> at room temperature. The starting *o*-alkynylaldehyde **10**, bearing the electron-donating –CH<sub>3</sub> group in *para* position to the triple bond of the phenyl ring was found to be suitable to trigger the heterocyclization reaction, by the possible formation of the intermediates **A,B**, and provided the desired pyrazole ester **12** in 64% yield. Also the *o*-alkynylaldehyde **11**, featuring the electron-withdrawing 2,4-dichlorophenyl group proved to be favourable for the reaction, even if the corresponding pyrazole ester **13** was obtained in 49% yield. The hydrolysis of **12,13** with NaOH in THF afforded the acid precursors **14,15** in almost quantitative yield. Finally, the acids **14** and **15** were treated with pivaloyl chloride and then with the appropriate amine to provide the desired carboxamides **8a-k** (23-76% yield).

<<Insert Scheme 1>>

### 3. Results and discussion

#### 3.1. Cannabinoid receptor binding studies

The CB<sub>1</sub> and CB<sub>2</sub> receptor binding affinities of the novel pyrazolo[5,1-*f*][1,6]naphthyridine derivatives **8a-k** were evaluated by radioligand binding assays performed by using transfected human CB<sub>1</sub> and CB<sub>2</sub> Chinese hamster ovary (CHO) cells. [<sup>3</sup>H]CP-55,940 was employed as radiolabeled ligand. The experimental data (IC<sub>50</sub> values) were converted into K<sub>i</sub> values.<sup>34</sup> The receptor affinities are shown in Table 1. For comparison, the K<sub>i</sub> value of the mixed CB<sub>1</sub>/CB<sub>2</sub> ligand WIN 55,212-2 is reported. Our initial results showed that the introduction of a fenchyl group at the C<sub>2</sub> carboxamide portion in combination with a *p*-tolyl group at the C<sub>5</sub> position of the pyrazolo[5,1-*f*][1,6]naphthyridine scaffold gave compound **8a** endowed with negligible affinity for CB<sub>1</sub>R (K<sub>i</sub>CB<sub>1</sub> = 2200 nM) and low affinity for CB<sub>2</sub>R (K<sub>i</sub>CB<sub>2</sub> = 800 nM). Further, replacement of the *N*-fenchyl moiety of **8a** with *N*-piperidinyl (**8b**) and *N*-cyclohexyl (**8c**) tail-pieces resulted in total loss of affinity for both CB<sub>1</sub> and CB<sub>2</sub>Rs. To further explore whether improvements in CBR-affinity might be obtained by modifying the C<sub>2</sub>-carboxamide side group, we next synthesized a small library of four monoterpene derivatives (**8d-g**) and two adamantane compounds (**8h,i**). Interestingly, all these compounds exhibited improved CB<sub>2</sub>R affinity, almost total loss of affinity for CB<sub>1</sub>R, and improved CB<sub>1</sub> to CB<sub>2</sub> selectivity than did **8a**. Among the monoterpene series, compound **8f**, featuring a bornyl group, emerged for its high CB<sub>2</sub>R

affinity (**8f**:  $K_i = 53\text{nM}$  versus **8a**:  $K_i = 800\text{ nM}$ ) and  $\text{CB}_1$  to  $\text{CB}_2$  selectivity (**8f**:  $K_i\text{CB}_1/K_i\text{CB}_2 = 132:1$  versus **8a**:  $K_i\text{CB}_1/K_i\text{CB}_2 = 2.7:1$ ). Concerning the adamantine derivatives, compound **8h** featuring a 1-adamantyl group, exhibited the higher  $\text{CB}_2\text{R}$  affinity and  $\text{CB}_1$  to  $\text{CB}_2$  selectivity among all the synthesized compounds (**8h**:  $K_i = 33\text{nM}$ ,  $K_i\text{CB}_1/K_i\text{CB}_2 = 173:1$ ). Finally, compound **8j**, derived from compound **8d** by replacing the *p*-tolyl group at the C<sub>5</sub>-position with a dichlorophenyl group, exhibited improved  $\text{CB}_2\text{R}$  affinity (**8j**:  $K_i = 67\text{ nM}$  versus **8d**:  $K_i = 120\text{ nM}$ ) and selectivity (**8j**:  $K_i\text{CB}_1/K_i\text{CB}_2 = > 149:1$  versus **8d**:  $K_i\text{CB}_1/K_i\text{CB}_2 = 83:1$ ), highlighting the versatility of the planar pyrazolo[5,1-*f*][1,6]naphthyridine scaffold to determine  $\text{CB}_2\text{R}$  affinity and selectivity.

<<Insert Table 1>>

### 3.2. Intrinsic activity by *in vitro* assay

The compounds **8f**, **8h**, and **8j** characterized by the best affinity and selectivity towards  $\text{CB}_2$  receptors were investigated to evaluate their activity as agonists or antagonists on  $\text{CB}_2$  receptors in functional assays. In particular their ability to affect forskolin-stimulated cAMP levels in human  $\text{CB}_2$  CHO cells has been evaluated and compared to WIN 55,212-2. As shown in Figure 4, the reference agonist WIN 55,212-2 (0.1  $\mu\text{M}$ ) was able to inhibit forskolin-stimulated cAMP levels of 52% and all the compounds under examination were able to antagonize this effect in the range of concentration 0.1-10  $\mu\text{M}$ , with the **8h** being the most potent compound, according to binding data.

To evaluate in more detail the potency of compounds to antagonize cAMP inhibition induced by WIN 55,212-2 a Schild analysis was performed. Compound **8h** shifted the concentration-response curve of WIN 55,212-2 to the right, in a concentration-dependent manner (Figure 5A). A Schild plot of the data gave a line with a slope near unity ( $1.05 \pm 0.06$ ) and  $K_B$  value of  $316 \pm 47\text{ nM}$  (Fig. 5B). Analogously, compounds **8f** and **8j** present a  $K_B$  value of  $505 \pm 61$  and  $650 \pm 74\text{ nM}$ , respectively. Therefore, the compounds investigated appear weaker in the functional assay respect to the binding test. However, these shifts have been repeatedly reported in the literature for different GPCRs and also for  $\text{CB}_2$  receptors.<sup>35</sup> Moreover, the values of  $\text{CB}_2$  affinity in binding assay and functional tests have not to be necessarily identical. What is interesting to note is that a good correlation between receptor affinity ( $K_i$ ) and efficacy ( $K_B$ ) was observed because the order of potency between the affinity and potency values is the same. Nevertheless, we could hypothesize that the discrepancy concerning the affinity values found between binding and functional test derive from the different experimental conditions between these assays, e.g. ionic strength of the buffer, time and temperature of the incubations.

Furthermore **8f** and **8j** ligands were able to increase forskolin-stimulated cAMP production at 1-10  $\mu\text{M}$ , whilst **8h** compound started its significant effect at 0.1  $\mu\text{M}$  (Fig. 6). These results

characterize the compounds **8f**, **8h**, and **8j** as antagonists/inverse agonists at **CB<sub>2</sub>R**. Accordingly, it has been shown that also the commercially available **CB<sub>2</sub>** receptor ligand **AM630** behaves as neutral antagonist, or agonist, or inverse agonist depending on the bioassay type or cell line.<sup>36</sup> This may be explained based on the two-state model theory of GPCRs in which ligands depending on their affinity for the receptor may shift it from an inactive to an active state, when they are agonists, or vice versa, in the case of inverse agonists. In addition, compounds not producing any shift in active/inactive receptor ratio are defined neutral antagonists.<sup>37</sup> Therefore, our compounds appear as inverse agonists in the absence of **WIN 55,212-2** while as antagonists in its presence.

<<Insert Figure 4>>

<<Insert Figure 5>>

<<Insert Figure 6>>

### 3.3. Molecular modeling studies

In this work, in order to rationalize the pharmacological results concerning the most promising derivatives **8f**, **8h** and **8j** and to refine our computational model, which could guide further synthetic efforts, docking studies on **8f**, **8h** and **8j** were also performed (see Supplementary material, Tab. 1). In this way, we disclosed the specific pattern of interactions probably related to the pyrazolo[5,1-*f*][1,6]naphthyridine scaffold as **CB<sub>2</sub>** inverse agonists.

This kind of approach relied on a ligand-based homology model of the human **CB<sub>2</sub>** receptor we previously built around the chemical scaffold of the potent ligand **4** (SR144528), revealing a pool of key residues involved in the antagonist binding.<sup>38</sup> Notably, our results were in agreement with those discussed by Montero and coworkers about the putative antagonist binding site of the h**CB<sub>2</sub>** receptor.<sup>39</sup> Thus, according to our calculations and also in agreement with recent data reported in literature, the interactions of the inverse agonists with the receptor included H-bonds at least with S165 for weaker compounds, or both the T114 and S165 residues for the most potent derivatives.<sup>35</sup>

In particular, the SR144528 4-chloro-3-methyl-phenyl and the benzyl group were projected toward two hydrophobic pockets including L195, Y190, W194 and I110, L169, respectively. On the other hand, the fenchyl portion was surrounded by L160, V164, F197 and F202.

These findings allowed us to highlight the key role played by a bulky group in proximity of the third hydrophobic pocket in terms of selectivity issue. Indeed, the **CB<sub>2</sub>** V164 corresponds to an isoleucine



residue at the **CB<sub>1</sub>** protein, determining specific steric requirements for the binding to **CB<sub>1</sub>** and, therefore, for **CB<sub>2</sub>** selectivity. Notably, all these data are also supported by the computational studies we performed within a series of tricyclic pyrazole carboxamides as **CB<sub>2</sub>** inverse agonists.<sup>40</sup> According to our calculations, in this study, compounds **8f**, **8h** and **8j** share quite a similar behaviour if compared with that of SR144528, displaying an overall pattern of interactions including the required H-bonds and a number of  $\pi$ - $\pi$  stacking and Van der Waals contacts with the three aforementioned hydrophobic pockets (see Supplementary material, Fig. 9).

More in details, the most potent **8h** derivative shows one H-bond between the carbonyl oxygen atom and the S165 side-chain, in tandem with a second H-bond with the T114 backbone (Fig. 7).

<<Insert Figure 7>>

In addition, the phenyl ring is engaged in  $\pi$ - $\pi$  stacking with W194 while the tricyclic core proves to mimic the reference compound fenchyl group. Accordingly, **8h** is characterized by a very favourable selectivity profile. Furthermore, the Q substituent is able to play the same role of the SR144528 phenyl and benzyl substituents, partially occupying the region delimited by L107, I110, L169, L182 and Y190.

As shown in Figure 8 and 9, the related analogues **8f** and **8j** display a highly similar binding mode, with the exception of the Q group on **8j**. Indeed, the presence of a methylene between the nitrogen atom and the cycloaliphatic moiety increases the Q group flexibility, thus it moves quite far from the receptor crevice surrounded by L107, I110 and L182.

<<Insert Figure 8>>

<<Insert Figure 9>>

These results confirm that a promising affinity profile could be obtained especially performing a proper set of H-bonds with T114 and S165, while selectivity appears to be strictly related to the hindered groups interacting with V164. On this basis, the computational studies here discussed are expected to pave the way for a further design process and for the filtering of new more potent and selective ligands.

### 3.4. *In silico* evaluation of pharmacokinetic properties

The computationally-driven prediction of descriptors related to absorption, distribution, metabolism, excretion and toxicity properties (ADMET) allows to rely on a useful strategy accelerating the lead compound discovery process.<sup>41</sup>

In this work, for the newly synthesized derivatives **8f**, **8h**, **8j** and also for **4**, a series of ADMET properties were calculated. In details, we took into account the logarithmic ratio of the octanol-water partitioning coefficient (cLogP), extent of blood-brain barrier permeation (LogBB), rate of passive diffusion-permeability (LogPS), human intestinal absorption (HIA), volume of distribution (Vd), the role played by plasmatic protein binding (%PPB) and by the compound affinity toward the human serum albumin (LogK<sub>a</sub><sup>HSA</sup>), and an overall perspective of the molecule oral bioavailability (%F).

In addition, we evaluated a number of descriptors predicting for metabolism and toxicity profiles, including the compound potential behaviour as P-glycoprotein substrate, the ability to act as cytochrome P450 3A4 inhibitor or substrate, the median lethal dose (LD<sub>50</sub>) related to oral administration.

As shown in Table 2, all the compounds are characterized by a better favourable profile in terms of lipophilicity, being the calculated cLogP within 5 (Lipinski rules) for **8f** and **8h** and, in any case, lower than that displayed by the reference compound **4**, being insoluble in water (solubility ≤ 0.05 mg/ml). Notably, all of them, with the exception of **8j**, show an overall adequate blood-brain barrier permeation, showing LogBB and/or LogPS values falling in the recommended ranges (0 < LogBB < 1.5; -3 < LogPS < -1). Only **8j** was characterized by a predicted weak ability to pass at the central nervous system. All of them are able to be fully adsorbed at the human intestinal membrane (HIA). The calculated volume of distribution values and the potential binding to the plasmatic proteins fall in the allowed ranges, being in any case consistent with those shown for **4**. As an overall consequence, compounds **8f** and **8h** are endowed with a favourable or acceptable bioavailability profile (%F), especially in comparison with **4**.

<<Insert Table 2>>

Based on Table 3, none of the compounds here proposed should be substrate of the P-glycoprotein, or be involved in cytochrome P450 3A4 inhibition. On the contrary, they should be substrate for the enzyme, showing comparable values with those displayed by **4**. Finally, **8f** and **8h** exhibit an acceptable toxicity profile, being the estimated LD<sub>50</sub> in the range of 320-430 mg/kg for mouse after oral administration, a value highly comparable with that calculated for the reference compound.

<<Insert Table 3>>

## 4. Conclusion

In conclusion, a small series of pyrazolo[5,1-*f*][1,6]naphthyridines **8** have been designed and synthesized for **CB<sub>1</sub>/CB<sub>2</sub>R** interaction. Among the synthesized compounds, **8f**, **8h** and **8j** exhibited affinity levels for **CB<sub>2</sub>R** in the near nM range (33-67 nM) with a high degree of selectivity for **CB<sub>2</sub>** compared to **CB<sub>1</sub>** ( $K_i\text{CB}_1/K_i\text{CB}_2$ : 132-173). According to *in vitro* assays based on the effects of forskolin-stimulated cAMP levels in human **CB<sub>2</sub>** CHO cells, compounds **8f**, **8h** and **8j** act as antagonist/inverse agonists. Docking studies carried out on such compounds and the reference **4** (SR144528) disclosed the specific pattern of interactions probably related to the pyrazolo[5,1-*f*][1,6]naphthyridine scaffold as **CB<sub>2</sub>** inverse agonists. Our preliminary results point out the versatility of the planar pyrazolo[5,1-*f*][1,6]naphthyridine architecture to provide novel chemical entities for **CB<sub>2</sub>R** interaction and pave the way for a further design process and for the filtering of new more potent and selective **CB<sub>2</sub>** ligands. Further work on this interesting class of **CB<sub>2</sub>R** ligands will be disclosed in due course.

## 5. Experimental protocols

### 5.1. Chemistry.

#### 5.1.1. General methods

Melting points were obtained on a Koffler melting point apparatus and are uncorrected. IR spectra were recorded as KBr pellets with a Jasco FT/IR 460 plus spectrophotometer and are expressed in  $\nu$  ( $\text{cm}^{-1}$ ).  $^1\text{H}$  NMR spectra were taken on a Bruker AVANCE III Nanobody 400 MHz spectrometer with  $^1\text{H}$  and  $^{13}\text{C}$  being observed at 400 and 100.6 MHz, respectively. Chemical shifts for  $^1\text{H}$  and  $^{13}\text{C}$  NMR spectra were reported in  $\delta$  (ppm) downfield from tetramethylsilane, and coupling constants ( $J$ ) were expressed in Hertz. Multiplicities are recorded as s (singlet), br s (broad singlet), d (doublet), t (triplet), dd (doublet of doublets), ddd (doublet of doublet douplets), m (multiplet). Atmospheric Pressure Ionization Electrospray (API-ES) mass spectra were obtained on an Agilent 1100 series LC/MSD spectrometer. Elemental analyses were performed with a PerkinElmer 2400 analyzer, and results were within  $\pm 0.40\%$  of the calculated values. Microwave experiments were carried out by a Biotage Initiator-8-microwave system (max pressure 20 bar, IR temperature sensor). TLC was performed on Merck silica gel 60 TLC plates F254 and visualized using UV. Flash chromatography (FC) was performed using Merck silica gel 60 (230-400 mesh ASTM).

2-Bromonicotinaldehyde (**9**), amines and *p*-tolylacetylene were purchased by Sigma-Aldrich®. Fenchylamine<sup>42</sup> and 2,4-dichlorophenylacetylene<sup>43</sup> were synthesized according to literature procedure. Title compounds **8a**, **8h** and **8i** were tested as hydrochloride salts.

### 5.1.2. General procedure I. Synthesis of *o*-alkynylaldehydes (**10,11**)

A mixture of 2-bromonicotinaldehyde (**9**) (1eq, 2.68 mmol), the appropriate alkyne (1.2 eq, 3.22 mmol), Pd(PPh<sub>3</sub>)<sub>2</sub>Cl<sub>2</sub> (0.04 eq, 0.11 mmol), CuI (0.07 eq, 0.20 mmol), Et<sub>3</sub>N (1.5 eq, 4.02 mmol), in dry DMF (16 mL), was stirred under argon atmosphere using microwave irradiation at 60 °C for 20 min. The reaction mixture was cooled to room temperature, quenched with Et<sub>2</sub>O (200 ml) and the solid filtered off. The organic solution was evaporated to afford a crude residue which was purified by FC (petroleum ether/AcOEt 8:2).

#### 5.1.2.1. 2-(*p*-Tolylethynyl)nicotinaldehyde (**10**)<sup>44</sup>

General procedure I was used to convert **9** and *p*-tolylacetylene into the title product. Yellow solid (0.485 g, 82%); R<sub>f</sub> 0.37 (AcOEt/petroleum ether 2:8); mp 97-99.°C (Lit. 96-100 °C); <sup>1</sup>H-NMR (CDCl<sub>3</sub>) 2.39 (s, 3H), 7.20 (d, *J* = 7.6 Hz, 2H), 7.38 (dd, *J* = 4.8 Hz, *J* = 7.6 Hz, 1H), 7.63 (d, *J* = 7.6 Hz, 2H), 8.20 (d, *J* = 8.0 Hz, 1H), 8.81 (d, *J* = 4.8 Hz, 1H), 10.66 (s, 1H); <sup>13</sup>C NMR (CDCl<sub>3</sub>) 21.8, 84.4, 96.7, 118.3, 123.2, 129.5, 131.8, 132.3, 134.9, 140.5, 146.4, 154.6, 191.1; API-ES *m/z*: [M+H]<sup>+</sup> calcd for C<sub>15</sub>H<sub>12</sub>NO: 222.1, found: 222.1.

#### 5.1.2.2. 2-((2,4-Dichlorophenyl)ethynyl)nicotinaldehyde (**11**)

General procedure I was used to convert **9** and 2,4-dichlorophenylacetylene into the title product. Cream solid (0.376 g, 51%); R<sub>f</sub> 0.28 (AcOEt/petroleum ether 2:8); mp 160-162 °C; <sup>1</sup>H-NMR (CDCl<sub>3</sub>) 7.29 (dd, *J* = 1.6 Hz, *J* = 8.4 Hz, 1H), 7.44 (dd, *J* = 4.8 Hz, *J* = 8.0 Hz, 1H), 7.49 (d, *J* = 1.6 Hz, 1H), 7.62 (d, *J* = 8.4 Hz, 1H), 8.23 (dd, *J* = 1.2 Hz, *J* = 8.0 Hz, 1H), 8.84 (dd, *J* = 1.6 Hz, *J* = 4.8 Hz, 1H), 10.73 (s, 1H); <sup>13</sup>C NMR (CDCl<sub>3</sub>) 90.3, 91.4, 120.2, 123.8, 127.5, 129.8, 132.4, 134.7, 134.9, 136.6, 137.6, 145.6, 154.7, 190.9; API-ES *m/z*: [M+H]<sup>+</sup> calcd for C<sub>14</sub>H<sub>8</sub>Cl<sub>2</sub>NO: 275.9, found: 275.8. **Anal.** (C<sub>14</sub>H<sub>7</sub>Cl<sub>2</sub>NO) C, H, N.

### 5.1.3. General procedure II. Synthesis of pyrazole esters (**12,13**)

A mixture of the appropriate *o*-alkynylaldehyde (1 eq, 0.452 mmol), PTSH (1.05 eq, 0.474 mmol), AgOTf (0.1 eq, 0.0452 mmol), DL-proline (0.1 eq, 0.0452 mmol), in dry EtOH (4 mL) was stirred at room temperature for 10 min. Ethyl pyruvate (10 eq, 4.520 mmol) was added, and the whole heated by microwave irradiation to 60 °C for 3.5 h. The reaction mixture was cooled to room temperature;

Na<sub>2</sub>CO<sub>3</sub> (6 eq, 2.712 mmol) was added and the mixture stirred at room temperature for 12 h. The solvent was evaporated to afford a crude residue which was purified by FC (petroleum ether/AcOEt 6:4).

#### 5.1.3.1. Ethyl 5-(*p*-tolyl)pyrazolo[5,1-*ff*][1,6]naphthyridine-2-carboxylate (**12**)

General procedure II was used to convert **10** into the title product. White solid (0.100 g, 64%); R<sub>f</sub> 0.34 (AcOEt/petroleum ether 4:6); mp 176-179.°C; IR 1716 (CO); <sup>1</sup>H NMR (CDCl<sub>3</sub>) 1.44 (t, *J* = 7.2 Hz, 3H), 2.46 (s, 3H), 4.46 (q, *J* = 7.2 Hz, 2H), 7.35 (d, *J* = 8.0 Hz, 2H), 7.46 (s, 1H), 7.50 (dd, *J* = 4.8 Hz, *J* = 8.0 Hz, 1H), 7.66 (s, 1H), 7.90 (d, *J* = 8.0 Hz, 2H), 8.40 (dd, *J* = 1.6 Hz, *J* = 8.0 Hz, 1H), 8.90 (dd, *J* = 1.6 Hz, *J* = 4.8 Hz, 1H); <sup>13</sup>C NMR (CDCl<sub>3</sub>) 14.5, 21.6, 61.5, 102.0, 115.8, 119.8, 122.3, 129.4, 129.6, 129.7, 131.3, 139.7, 140.4, 142.6, 145.1, 146.4, 151.4, 162.7; API-ES *m/z*: [M+H]<sup>+</sup> calcd for C<sub>20</sub>H<sub>18</sub>N<sub>3</sub>O<sub>2</sub>: 332.1, found: 332.1. **Anal.** (C<sub>20</sub>H<sub>17</sub>N<sub>3</sub>O<sub>2</sub>) C, H, N.

#### 5.1.3.2. Ethyl 5-(2,4-dichlorophenyl)pyrazolo[5,1-*ff*][1,6]naphthyridine-2-carboxylate (**13**)

General procedure II was used to convert **11** into the title product. White solid (0.085 g, 49%); R<sub>f</sub> 0.31 (AcOEt/petroleum ether 4:6); mp 231-234.°C; IR 1729 (CO); <sup>1</sup>H NMR (DMSO-*d*<sub>6</sub>) 1.31 (t, *J* = 6.4 Hz, 3H), 4.34 (q, *J* = 6.4 Hz, 2H), 7.49 (s, 1H), 7.68 (d, *J* = 8.0 Hz, 1H), 7.77 (d, *J* = 8.0 Hz, 2H), 7.91 (s, 1H), 8.06 (s, 1H), 8.91-9.00 (m, 2H); <sup>13</sup>C NMR (DMSO-*d*<sub>6</sub>) 14.2, 60.9, 103.1, 117.3, 119.9, 123.6, 127.8, 129.2, 130.7, 132.2, 133.5, 134.6, 135.5, 137.7, 138.7, 144.5, 144.8, 151.7, 161.6; API-ES *m/z*: [M+H]<sup>+</sup> calcd for C<sub>19</sub>H<sub>14</sub>Cl<sub>2</sub>N<sub>3</sub>O<sub>2</sub>: 386.0, found: 386.3. **Anal.** (C<sub>19</sub>H<sub>13</sub>Cl<sub>2</sub>N<sub>3</sub>O<sub>2</sub>) C, H, N.

#### 5.1.4. General procedure III. Synthesis of pyrazole acids (**14,15**)

To a solution of appropriate pyrazole ester (1 eq, 1.41 mmol) in THF (10 ml), 10% aqueous NaOH solution (10 ml) was added dropwise, and the whole stirred at 40 °C for 3h. The solution was cooled at room temperature and neutralized with 4N HCl. The solid was filtered, washed with acetone to give a crude product which was used in the following step with no further purification.

#### 5.1.4.1. 5-(*p*-tolyl)pyrazolo[5,1-*ff*][1,6]naphthyridine-2-carboxylic acid (**14**)

General procedure III was used to convert **12** into the title product. White solid (0.443 g, 95%). IR 3422 (OH), 1636 (CO).

#### 5.1.4.2. 5-(2,4-Dichlorophenyl)pyrazolo[5,1-*ff*][1,6]naphthyridine-2-carboxylic acid (**15**)

General procedure III was used to convert **13** into the title product. Yellow solid (0.352 g, 70%). IR 3448 (OH), 1718 (CO).

#### 5.1.5. General procedure IV. Synthesis of carboxamides (**8a-k**)

A solution of appropriate acid (1 eq. 0.495 mmol) and Et<sub>3</sub>N (3 eq. 1.50 mmol) in dry CH<sub>2</sub>Cl<sub>2</sub> (10 mL) was cooled at 0 °C; pivaloyl chloride (2.5 eq. 1.237 mmol) was dropwise added and the whole warmed to room temperature and stirred for 2 h. This mixture was dropwise added at 0 °C to a solution of appropriate amine or hydrazine (0.9 eq. 0.990 mmol) and Et<sub>3</sub>N (1.5 eq. 1.500 mmol) in dry CH<sub>2</sub>Cl<sub>2</sub> (5 mL) and the whole stirred at room temperature for 2.5 h. The reaction mixture was quenched with an aqueous saturated solution of NH<sub>4</sub>Cl and extracted with CH<sub>2</sub>Cl<sub>2</sub>. The organic phase was dried (Na<sub>2</sub>SO<sub>4</sub>) and evaporated to give a crude residue which was purified by FC (petroleum ether/AcOEt 3:7).

##### 5.1.5.1. *N*-Fenchyl-5-(*p*-tolyl)pyrazolo[5,1-*f*][1,6]naphthyridine-2-carboxamide (**8a**)

General procedure IV was used to convert **14** and fenchylamine into the title product. White solid (0.050 g, 23%). R<sub>f</sub> 0.49 (AcOEt/petroleum ether 7:3); mp 220-222 °C; IR 3404 (NH), 1673 (CO); <sup>1</sup>H NMR (CDCl<sub>3</sub>) 0.86 (s, 3H), 1.11 (s, 3H), 1.14-1.22 (m, 4H), 1.23-1.30 (m, 1H), 1.29-1.39 (m, 1H), 1.43-1.55 (m, 1H), 1.66-1.77 (m, 2H), 1.80 (d, *J* = 2.8 Hz, 1H), 2.49 (s, 3H), 3.83 (d, *J* = 9.6 Hz, 1H), 7.23 (d, *J* = 9.6 Hz, 1H), 7.36 (d, *J* = 8.0 Hz, 2H), 7.46 (s, 1H), 7.50 (dd, *J* = 4.4 Hz, *J* = 8.0 Hz, 1H), 7.65 (s, 1H), 7.93 (d, *J* = 8.0 Hz, 2H), 8.42 (d, *J* = 8.0 Hz, 1H), 8.89 (d, *J* = 4.4 Hz, 1H); <sup>13</sup>C NMR (CDCl<sub>3</sub>) 19.8, 21.3, 21.7, 26.1, 27.3, 31.1, 39.7, 42.8, 48.3, 48.9, 63.3, 99.7, 115.2, 119.9, 122.4, 129.0, 129.6, 129.8, 131.5, 140.2, 140.4, 141.9, 146.4, 147.9, 151.3, 162.5; API-ES *m/z*: [M+H]<sup>+</sup> calcd for C<sub>28</sub>H<sub>31</sub>N<sub>4</sub>O: 439.2, found: 439.2. Anal. (C<sub>28</sub>H<sub>30</sub>N<sub>4</sub>O) C, H, N.

##### 5.1.5.2. *N*-(piperidin-1-yl)-5-(*p*-tolyl)pyrazolo[5,1-*f*][1,6]naphthyridine-2-carboxamide (**8b**)

General procedure IV was used to convert **14** and *N*-aminopiperidine into the title product. Cream solid (0.078 g, 41%). R<sub>f</sub> 0.11 (AcOEt/petroleum ether 7:3); mp 207 °C; IR 3398 (NH), 1687 (CO); <sup>1</sup>H NMR (CDCl<sub>3</sub>) 1.41-1.49 (m, 2H), 1.71-1.79 (m, 4H), 2.50 (s, 3H), 2.90 (t, *J* = 5.2 Hz, 4H), 7.39 (d, *J* = 8.0 Hz, 2H), 7.41 (s, 1H), 7.51 (dd, *J* = 4.4 Hz, *J* = 8.0 Hz, 1H), 7.72 (s, 1H), 7.76 (s, 1H), 7.84 (d, *J* = 8.0 Hz, 2H), 8.41 (dd, *J* = 1.6 Hz, *J* = 8.0 Hz, 1H), 8.89 (dd, *J* = 1.6 Hz, *J* = 4.4 Hz, 1H); <sup>13</sup>C NMR (CDCl<sub>3</sub>) 21.7, 23.4, 25.5, 57.0, 100.6, 115.6, 119.8, 122.5, 129.3, 129.5, 129.9, 131.6, 140.0, 140.4, 142.0, 146.3, 147.3, 151.4, 159.3; API-ES *m/z*: [M+H]<sup>+</sup> calcd for C<sub>23</sub>H<sub>24</sub>N<sub>5</sub>O: 386.2, found: 386.0. Anal. (C<sub>23</sub>H<sub>23</sub>N<sub>5</sub>O) C, H, N.

#### 5.1.5.3. *N*-Cyclohexyl-5-(*p*-tolyl)pyrazolo[5,1-*f*][1,6]naphthyridine-2-carboxamide (**8c**)

General procedure IV was used to convert **14** and *N*-cyclohexylamine into the title product. White solid (0.051 g, 27%).  $R_f$  0.50 (AcOEt/petroleum ether 7:3); mp 229-230 °C; IR 3406 (NH), 1670 (CO);  $^1\text{H}$  NMR ( $\text{CDCl}_3$ ) 1.16-1.32 (m, 3H), 1.35-1.48 (m, 2H), 1.60-1.69 (m, 1H), 1.71-1.80 (m, 2H), 1.97-2.06 (m, 2H), 2.49 (s, 3H), 3.92-4.05 (m, 1H), 6.89 (d,  $J = 8.0$  Hz, 1H), 7.38 (d,  $J = 8.0$  Hz, 2H), 7.40 (s, 1H), 7.50 (dd,  $J = 4.8$  Hz,  $J = 8.0$  Hz, 1H), 7.67 (s, 1H), 7.85 (d,  $J = 8.0$  Hz, 2H), 8.41 (d,  $J = 8.0$  Hz, 1H), 8.88 (d,  $J = 3.20$  Hz, 1H);  $^{13}\text{C}$  NMR ( $\text{CDCl}_3$ ) 21.6, 25.1, 25.7, 33.3, 48.3, 100.1, 115.4, 119.9, 122.4, 129.3, 129.5, 129.9, 131.5, 140.1, 140.3, 142.1, 146.3, 148.2, 151.3, 161.0; API-ES  $m/z$ :  $[\text{M}+\text{H}]^+$  calcd for  $\text{C}_{24}\text{H}_{25}\text{N}_4\text{O}$ : 385.2, found: 385.5. Anal. ( $\text{C}_{24}\text{H}_{24}\text{N}_4\text{O}$ ) C, H, N.

#### 5.1.5.4. *N*-Myrtanyl-5-(*p*-tolyl)pyrazolo[5,1-*f*][1,6]naphthyridine-2-carboxamide (**8d**)

General procedure IV was used to convert **14** and myrtanylamine into the title product. White solid (0.128, 59%).  $R_f$  0.53 (AcOEt/petroleum ether 7:3); mp 164-166 °C; IR 3448 (NH), 1670 (CO);  $^1\text{H}$  NMR ( $\text{CDCl}_3$ ) 0.91 (d,  $J = 9.6$  Hz, 1H), 1.10 (s, 3H), 1.21 (s, 3H), 1.51-1.62 (m, 1H); 1.85-2.01 (m, 5H), 2.28-2.40 (m, 2H), 2.49 (s, 3H), 3.41-3.53 (m, 2H), 7.08 (t,  $J = 5.8$  Hz, 1H), 7.38 (d,  $J = 8.0$  Hz, 2H), 7.41 (s, 1H), 7.51 (dd,  $J = 4.0$  Hz,  $J = 8.0$  Hz, 1H), 7.68 (s, 1H), 7.85 (d,  $J = 8.0$  Hz, 2H), 8.42 (dd,  $J = 0.8$  Hz,  $J = 8.0$  Hz, 1H), 8.89 (d,  $J = 3.2$  Hz, 1H);  $^{13}\text{C}$  NMR ( $\text{CDCl}_3$ ) 19.9, 21.66, 23.4, 26.2, 28.1, 33.4, 38.9, 41.5, 41.7, 44.0, 44.9, 100.1, 115.4, 119.9, 122.4, 129.3, 129.6, 129.9, 131.6, 140.1, 140.4, 142.1, 146.3, 148.0, 151.3, 161.9; API-ES  $m/z$ :  $[\text{M}+\text{H}]^+$  calcd for  $\text{C}_{28}\text{H}_{31}\text{N}_4\text{O}$ : 439.2, found: 439.5. Anal. ( $\text{C}_{28}\text{H}_{30}\text{N}_4\text{O}$ ) C, H, N.

#### 5.1.5.5. *N*-Isopinocampheyl-5-(*p*-tolyl)pyrazolo[5,1-*f*][1,6]naphthyridine-2-carboxamide (**8e**)

General procedure IV was used to convert **14** and isopinocampheylamine into the title product. Yellow solid (0.074 g, 34%).  $R_f$  0.40 (AcOEt/petroleum ether 7:3); mp 215 °C; IR 3402 (NH), 1662 (CO);  $^1\text{H}$  NMR ( $\text{CDCl}_3$ ) 0.95 (d,  $J = 10.0$  Hz, 1H), 1.11 (s, 3H), 1.17 (d,  $J = 7.2$  Hz, 3H), 1.25 (s, 3H), 1.68 (ddd,  $J = 2.0$  Hz,  $J = 6.0$  Hz,  $J = 14.0$  Hz, 1H), 1.87 (t,  $J = 5.6$  Hz, 1H), 1.93 (t,  $J = 7.0$  Hz, 1H), 1.96-2.02 (m, 1H), 2.40-2.48 (m, 1H), 2.50 (s, 3H), 2.63-2.73 (m, 1H), 4.45-4.56 (m, 1H), 6.89 (d,  $J = 9.2$  Hz, 1H), 7.39 (d,  $J = 8.0$  Hz, 2H), 7.42 (s, 1H), 7.51 (dd,  $J = 4.0$  Hz,  $J = 8.0$  Hz, 1H), 7.69 (s, 1H), 7.87 (d,  $J = 8.0$  Hz, 2H), 8.43 (d,  $J = 8.0$  Hz, 1H), 8.90 (d,  $J = 4.0$  Hz, 1H);  $^{13}\text{C}$  NMR ( $\text{CDCl}_3$ ) 21.0, 21.7, 23.6, 28.2, 35.3, 37.1, 38.6, 41.8, 46.2, 47.9, 48.0, 100.2, 115.5, 119.9, 122.4, 129.3, 129.5, 129.9, 131.5, 140.1, 140.4, 142.1, 146.3, 148.1, 151.3, 161.4; API-ES  $m/z$ :  $[\text{M}+\text{H}]^+$  calcd for  $\text{C}_{28}\text{H}_{31}\text{N}_4\text{O}$ : 439.2, found: 439.4. Anal. ( $\text{C}_{28}\text{H}_{30}\text{N}_4\text{O}$ ) C, H, N.

#### 5.1.5.6. *N*-Bornyl-5-(*p*-tolyl)pyrazolo[5,1-*f*][1,6]naphthyridine-2-carboxamide (**8f**)



General procedure IV was used to convert **14** and bornylamine into the title product. Yellow solid (0.093 g, 43%).  $R_f$  0.52 (AcOEt/petroleum ether 7:3); mp 224-225 °C; IR 3390 (NH), 1676 (CO);  $^1\text{H}$  NMR ( $\text{CDCl}_3$ ) 0.90 (s, 3H), 0.91 (s, 3H), 0.95 (dd,  $J = 4.4$  Hz,  $J = 13.6$  Hz, 1H), 1.01 (s, 3H), 1.18-1.28 (m, 1H), 1.38-1.50 (m, 1H), 1.55-1.65 (m, 1H), 1.71 (t,  $J = 4.4$  Hz, 1H), 1.76-1.88 (m, 1H), 2.37-2.47 (m, 1H), 2.49 (s, 3H), 4.41-4.50 (m, 1H), 7.17 (d,  $J = 9.2$  Hz, 1H), 7.37 (d,  $J = 8.0$  Hz, 2H), 7.45 (s, 1H), 7.51 (dd,  $J = 4.4$  Hz,  $J = 8.0$  Hz, 1H), 7.66 (s, 1H), 7.92 (d,  $J = 8.0$  Hz, 2H), 8.42 (d,  $J = 8.0$  Hz, 1H), 8.90 (dd,  $J = 1.2$  Hz,  $J = 4.4$  Hz, 1H);  $^{13}\text{C}$  NMR (101 MHz,  $\text{CDCl}_3$ ): 13.9, 18.9, 20.0, 21.7, 28.2, 28.5, 37.7, 45.2, 48.3, 50.0, 53.7, 99.9, 115.2, 119.9, 122.4, 129.1, 129.6, 129.8, 131.6, 140.2, 140.5, 142.0, 146.4, 148.0, 151.3, 162.0; API-ES  $m/z$ :  $[\text{M}+\text{H}]^+$  calcd for  $\text{C}_{28}\text{H}_{31}\text{N}_4\text{O}$ : 439.2, found: 439.2. Anal. ( $\text{C}_{28}\text{H}_{30}\text{N}_4\text{O}$ ) C, H, N.

#### 5.1.5.7. *N*-Menthyl-5-(*p*-tolyl)pyrazolo[5,1-*f*][1,6]naphthyridine-2-carboxamide (**8g**)

General procedure IV was used to convert **14** and menthylamine into the title product. White solid (0.165 g, 76%).  $R_f$  0.58 (AcOEt/petroleum ether 7:3); mp 151-152 °C; IR 3399 (NH), 1664 (CO);  $^1\text{H}$  NMR ( $\text{CDCl}_3$ ) 0.85-0.93 (m, 11H), 1.11-1.23 (m, 2H), 1.49-1.60 (m, 1H), 1.66-1.77 (m, 2H), 1.88-2.01 (m, 1H), 2.02-2.11 (m, 1H), 2.50 (s, 3H), 3.93-4.05 (m, 1H), 6.75 (d,  $J = 9.6$  Hz, 1H), 7.38 (d,  $J = 8.0$  Hz, 2H), 7.41 (s, 1H), 7.51 (dd,  $J = 4.4$  Hz,  $J = 8.0$  Hz, 1H), 7.68 (s, 1H), 7.86 (d,  $J = 8.0$  Hz, 2H), 8.41 (d,  $J = 8.0$  Hz, 1H), 8.89 (d,  $J = 4.4$  Hz, 1H);  $^{13}\text{C}$  NMR ( $\text{CDCl}_3$ ) 16.8, 21.1, 21.7, 22.3, 24.5, 27.3, 32.1, 34.7, 43.1, 48.2, 50.1, 100.1, 115.4, 119.9, 122.4, 129.3, 129.5, 130.0, 131.5, 140.1, 140.3, 142.1, 146.3, 148.1, 151.3, 161.2; API-ES  $m/z$ :  $[\text{M}+\text{H}]^+$  calcd for  $\text{C}_{28}\text{H}_{33}\text{N}_4\text{O}$ : 441.2, found: 441.5. Anal. ( $\text{C}_{28}\text{H}_{32}\text{N}_4\text{O}$ ) C, H, N.

#### 5.1.5.8. *N*-Adamant-1-yl-5-(*p*-tolyl)pyrazolo[5,1-*f*][1,6]naphthyridine-2-carboxamide (**8h**)

General procedure IV was used to convert **14** and 1-adamantylamine into the title product. White solid (0.12 g, 55%).  $R_f$  0.54 (AcOEt/petroleum ether 7:3); mp 238-240 °C; IR 3390 (NH), 1676 (CO);  $^1\text{H}$  NMR ( $\text{CDCl}_3$ ) 1.68-1.77 (m, 6H), 2.10-2.18 (m, 9H), 2.48 (s, 3H), 6.80 (s, 1H), 7.37 (d,  $J = 8.0$  Hz, 2H), 7.39 (s, 1H), 7.49 (dd,  $J = 4.4$  Hz,  $J = 8.0$  Hz, 1H), 7.61 (s, 1H), 7.85 (d,  $J = 8.0$  Hz, 2H), 8.40 (d,  $J = 8.0$  Hz, 1H), 8.88 (d,  $J = 4.4$  Hz, 1H);  $^{13}\text{C}$  NMR ( $\text{CDCl}_3$ ) 21.6, 29.6, 36.5, 41.7, 52.1, 99.8, 115.2, 119.9, 122.3, 129.2, 129.6, 129.9, 131.5, 140.1, 140.3, 142.0, 146.3, 148.9, 151.2, 160.9; API-ES  $m/z$ :  $[\text{M}+\text{H}]^+$  calcd for  $\text{C}_{28}\text{H}_{29}\text{N}_4\text{O}$ : 437.2, found: 437.5. Anal. ( $\text{C}_{28}\text{H}_{28}\text{N}_4\text{O}$ ) C, H, N.

#### 5.1.5.9. *N*-Adamant-2-yl-5-(*p*-tolyl)pyrazolo[5,1-*f*][1,6]naphthyridine-2-carboxamide (**8i**)

General procedure IV was used to convert **14** and 2-adamantylamine hydrochloride into the title product. White solid (0.153 g, 71%).  $R_f$  0.39 (AcOEt/petroleum ether 7:3); mp 218-220 °C; IR 3419



(NH), 1672 (CO); <sup>1</sup>H NMR (CDCl<sub>3</sub>) 1.68 (d, *J* = 12.8 Hz, 2H), 1.78 (s, 2H), 1.83-1.92 (m, 8H), 2.05 (s, 2H), 2.48 (s, 3H), 4.26 (d, *J* = 8.0 Hz, 1H), 7.36 (d, *J* = 8.0 Hz, 2H), 7.44 (s, 1H), 7.46-7.54 (m, 2H), 7.66 (s, 1H), 7.91 (d, *J* = 8.0 Hz, 2H), 8.41 (d, *J* = 8.0 Hz, 1H), 8.88 (d, *J* = 4.4 Hz, 1H); <sup>13</sup>C NMR (CDCl<sub>3</sub>) 21.6, 27.3, 27.5, 32.1, 32.2, 37.2, 37.7, 53.2, 99.8, 115.2, 119.9, 122.3, 129.1, 129.6, 129.8, 131.5, 140.1, 140.4, 142.0, 146.4, 148.1, 151.3, 161.0; API-ES *m/z*: [M+H]<sup>+</sup> calcd for C<sub>28</sub>H<sub>29</sub>N<sub>4</sub>O: 437.2, found: 437.4. Anal. (C<sub>28</sub>H<sub>28</sub>N<sub>4</sub>O) C, H, N.

#### 5.1.5.10. *N*-Myrtanyl-5-(2,4-dichlorophenyl)pyrazolo[5,1-*f*][1,6]naphthyridine-2-carboxamide (**8j**)

General procedure IV was used to convert **15** and myrtanylamine into the title product. White solid (0.090 g, 37%). *R<sub>f</sub>* 0.38 (AcOEt/petroleum ether 6:4); mp 216-218 °C; IR 3403 (NH), 1687 (CO); <sup>1</sup>H NMR (CDCl<sub>3</sub>) 0.90 (d, *J* = 9.6 Hz, 1H), 1.09 (s, 3H), 1.19 (s, 3H), 1.49-1.61 (m, 1H), 1.80-2.0 (m, 5H), 2.26-2.39 (m, 2H), 3.40-3.51 (m, 2H), 6.93 (t, *J* = 6.0 Hz, 1H), 7.36 (s, 1H), 7.46 (d, *J* = 8.4 Hz, 1H), 7.51-7.60 (m, 2H), 7.63 (s, 1H), 7.67 (s, 1H), 8.45 (d, *J* = 8.4 Hz, 1H), 8.92 (d, *J* = 4.4 Hz, 1H); <sup>13</sup>C NMR (CDCl<sub>3</sub>) 19.8, 23.4, 26.2, 28.1, 33.3, 38.8, 41.5, 41.6, 44.0, 45.0, 100.2, 117.2, 120.6, 123.0, 127.5, 130.1, 130.8, 131.7, 132.8, 135.6, 136.6, 138.4, 139.4, 145.7, 148.4, 151.4, 161.8; API-ES *m/z*: [M+H]<sup>+</sup> calcd for C<sub>27</sub>H<sub>27</sub>Cl<sub>2</sub>N<sub>4</sub>O: 494.2, found: 493.3. Anal. (C<sub>27</sub>H<sub>26</sub>Cl<sub>2</sub>N<sub>4</sub>O) C, H, N.

#### 5.1.5.11. *N*-Fenchyl-5-(2,4-dichlorophenyl)pyrazolo[5,1-*f*][1,6]naphthyridine-2-carboxamide (**8k**)

General procedure IV was used to convert **15** and fenchylamine into the title product. Cream solid (0.011 g, 44%). *R<sub>f</sub>* 0.42 (AcOEt/petroleum ether 6:4); mp 249-251 °C; IR 3387 (NH), 1671 (CO); <sup>1</sup>H NMR (CDCl<sub>3</sub>) 0.78 (s, 3H), 1.07 (s, 3H), 1.12-1.22 (m, 5H), 1.42-1.53 (m, 1H), 1.55-1.62 (m, 1H), 1.63-1.73 (m, 2H), 1.75-1.82 (m, 1H), 3.78 (d, *J* = 9.6 Hz, 1H), 7.07 (d, *J* = 10.0 Hz, 1H), 7.39 (s, 1H), 7.46 (d, *J* = 8.4 Hz, 1H), 7.54-7.60 (m, 2H), 7.62 (s, 1H), 7.65 (s, 1H), 8.46 (d, *J* = 8.4 Hz, 1H), 8.93 (d, *J* = 4.4 Hz, 1H); <sup>13</sup>C NMR (CDCl<sub>3</sub>): 19.8, 21.6, 26.1, 27.3, 31.1, 39.7, 42.7, 48.3, 48.9, 63.4, 99.9, 117.2, 120.6, 123.0, 127.4, 129.8, 130.8, 131.7, 132.8, 133.0, 136.7, 138.5, 139.4, 145.8, 148.4, 151.4, 162.3; API-ES *m/z*: [M+H]<sup>+</sup> calcd for C<sub>27</sub>H<sub>27</sub>Cl<sub>2</sub>N<sub>4</sub>O: 492.1, found: 493.4. Anal. (C<sub>27</sub>H<sub>26</sub>Cl<sub>2</sub>N<sub>4</sub>O) C, H, N.

## 5.2. Biological evaluation

### 5.2.1. Competition binding experiments for human CB<sub>1</sub> and CB<sub>2</sub> receptors

Competition binding experiments were carried out through [<sup>3</sup>H]CP-55,940 (specific activity, 180 Ci/mmol) provided by Perkin-Elmer Life and Analytical Sciences (U.S.). Human CB<sub>1</sub> and CB<sub>2</sub> receptors expressed in CHO cells were from Perkin-Elmer Life and Analytical Sciences (U.S.). All other reagents were derived from commercial sources.

CHO cells transfected with human **CB<sub>1</sub>** and **CB<sub>2</sub>** receptors were cultured in Ham's F12 containing 10% fetal bovine serum, penicillin (100 U/mL), streptomycin (100 µg/mL), and Geneticin (G418, 0.4 mg/ml) at 37 °C in 5% CO<sub>2</sub>/95% air.<sup>45</sup> Cellular membranes for binding experiments were obtained as previously described.<sup>45</sup> Briefly, the cells were scraped off in ice-cold hypotonic buffer (5 mM Tris-HCl, 2 mM EDTA, pH 7.4), homogenized with a Polytron, centrifuged for 10 min at 1000g, and the supernatant was further centrifuged for 30 min at 100000g. The pellet of membranes was diluted in 50 mM Tris-HCl buffer, 0.5% BSA (pH 7.4) containing 5 mM MgCl<sub>2</sub>, 2.5 mM EDTA or 1 mM EDTA for h**CB<sub>1</sub>** or h**CB<sub>2</sub>** receptor, respectively. Competition binding experiments were carried out with [<sup>3</sup>H]CP-55,940 and the examined compounds at different concentrations (1 nM to 10 µM) or WIN 55,212-2, the **CB<sub>1</sub>/CB<sub>2</sub>** standard agonist for 90 or 60 min at 30 °C for **CB<sub>1</sub>** or **CB<sub>2</sub>** receptors, respectively. Bound and free radioactivities were separated by filtering the assay mixture through Whatman GF/C glass fiber filters using a Brandel cell harvester (Brandel Instruments, Unterföhring, Germany). The filter bound radioactivity was counted on a Perkin-Elmer 2810 TR scintillation counter (Perkin-Elmer Life and Analytical Sciences, U.S.).

### 5.2.2. *cAMP assay for human **CB<sub>2</sub>** receptors*

CHO cells transfected with human **CB<sub>2</sub>** receptors were preincubated with 0.5 mM 4-(3-butoxy-4-methoxybenzyl)-2-imidazolidinone (Ro 20-1724) as a phosphodiesterase inhibitor and the effect of the novel CB compounds tested at increasing concentrations (0.1-10 µM) or WIN 55,212-2 (0.1 µM) was studied in the presence of forskolin (10 µM) by using the fluorimetric cAMP kit (cAMP direct immunoassay kit, ab65355, abcam) according to the manufacturer's instructions.

### 5.2.3. *Data analysis*

The protein concentration was evaluated by a Bio-Rad method<sup>46</sup> with bovine albumin as reference standard. Inhibitory binding constants,  $K_i$ , were obtained from the  $IC_{50}$  values following the Cheng and Prusoff equation:  $K_i = IC_{50}/(1 + [C]/K_D)$ , where [C] is the concentration of the radioligand and  $K_D$  its

dissociation constant (Cheng Prusoff).<sup>34</sup> A weighted nonlinear least-squares curve fitting program, LIGAND, was used for computer analysis of the inhibition experiments.<sup>47</sup> All the data are expressed as the mean  $\pm$  SEM of  $n = 4$  independent experiments. Statistical analysis of the data was performed using ANOVA followed by Dunnett's test.

### 5.3. Molecular modeling studies

Compounds **8f**, **8h** and **8j** were built, parameterized (Gasteiger-Huckel method) and energy minimized within MOE using MMFF94 forcefield.<sup>48</sup> Docking studies were performed using the previously built ligand-based human **CB<sub>2</sub>** homology model.<sup>38</sup> In particular, the **hCB<sub>2</sub>** inverse agonist binding site was defined taking into account any amino acids placed at 5Å distance far from the key residue S165, as described by mutagenesis data.<sup>49</sup> Successively, flexible docking studies were applied using the Surflex docking module implemented in Sybyl-X1.0.<sup>50</sup> Surflex-Dock uses an empirically derived scoring function based on the binding affinities of X-ray protein-ligand complexes.

The Surflex-Dock scoring function is a weighted sum of non-linear functions involving van der Waals surface distances between the appropriate pairs of exposed protein and ligand atoms, including hydrophobic, polar, repulsive, entropic and solvation and crash terms represented in terms of a total score conferred to any calculated conformer.

Then, the best docking geometry (selected on the basis of the SurFlex scoring functions) was refined by ligand/protein complex energy minimization (CHARMM27) by means of the MOE software. Finally, the protein-ligand complex stability was successfully assessed using a short  $\sim 1$  ps run of molecular dynamics (MD) at constant temperature, followed by an all-atom energy minimization (LowModeMD implemented in MOE software). In this way, an exhaustive conformational analysis of the ligand-receptor binding site complex was explored, as we already explained about other case studies for a preliminary evaluation of the derived docking poses.<sup>51</sup>

### 5.4. In silico evaluation of pharmacokinetic properties

The prediction of ADMET properties was performed using the Advanced Chemistry Development (ACD) Percepta platform ([www.acdlabs.com](http://www.acdlabs.com)).

Any ADMET descriptor was evaluated by Percepta, based on training libraries implemented in the software, which include a consistent pool of molecules whose pharmacokinetic and toxicity profiles are experimentally known.

## Conflict of interest

None of the authors have conflict of interest to declare.

## Acknowledgements

Authors acknowledge Regione Autonoma della Sardegna for economic support (grant n. CRP-26417, LR n. 7/2007 and INNOVA.RE- POR FESR 2007-2013)

## Appendix A. Supplementary data

Supplementary data related to this article can be found at...

## References

1. Di Marzo, V.; Bifulco, M.; De Petrocellis, L. *Nat. Rev. Drug Discov.* **2004**, *3*, 771.
2. Boyd, S. T. **2006**, *26*, 218S.
3. DiPatrizio, N. V.; Piomelli, D. *Trends Neurosci.* **2012**, *35*, 403.
4. Howlett, A. C.; Barth, F.; Bonner, T. I.; Cabral, G.; Casellas, P.; Devane, W. A.; Felder, C. C.; Herkenham, M.; Mackie, K.; Martin, B. R.; Mechoulam, R.; Pertwee, R. G. *Pharmacol. Rev.* **2002**, *54*, 161.
5. Reggio, P. H. *Curr. Med. Chem.* **2010**, *17*, 1468.
6. Gaoni, Y.; Mechoulam, R. *J. Am. Chem. Soc.* **1964**, *86*, 1646.
7. Matsuda, L. A.; Lolait, S. J.; Brownstein, M. J.; Young, A. C.; Bonner, T. I. *Nature* **1990**, *346*, 561.
8. Adams, I. B.; Martin, B. R. *Addiction* **1996**, *91*, 1585.
9. Pertwee, R. G.; Howlett, A. C.; Abood, M. E.; Alexander, S. P. H.; Di Marzo, V.; Elphick, M. R.; Greasley, P. J.; Hansen, H. S.; Kunos, G.; Mackie, K.; Mechoulam, R.; Ross, R. A. *Pharmacol. Rev.* **2010**, *62*, 588.
10. Freund, T. F.; Katona, I.; Piomelli, D. *Physiol. Rev.* **2003**, *83*, 1017.
11. Munro, S.; Thomas, K. L.; Abu-Shaar, M. *Nature*, **1993**, *365*, 61.
12. Galiegue, S.; Mary, S.; Marchand, J.; Dussossoy, D.; Carriere, D.; Carayon, P.; Bouaboula, M.; Shire, D.; Le Fur, G.; Casellas, P. *Eur. J. Biochem.* **1995**, *232*, 54.
13. Schatz, A. R.; Lee, M.; Condie, R. B.; Pulaski, J. T.; Kaminski, N. E. *Toxicol. Appl. Pharmacol.* **1997**, *142*, 278.
14. Lynn, A. B.; Herkenham, M. *J. Pharmacol. Exp. Ther.* **1994**, *268*, 1612.
15. (a) Van Sickle, M. D.; Duncan, M.; Kingsley, P. J.; Mouihate, A.; Urbani, P.; Mackie, K.; Stella, N.; Makriyannis, A.; Piomelli, D.; Davison, J. S.; Marnett, L. J.; Di Marzo, V.; Pittman, Q. J.; Patel, K.

- D.; Sharkey, K. A. *Science*, **2005**, *310*, 329. (b) Gong, J.-P.; Onaivi, E. S.; Ishiguro, H.; Liu, Q.-R.; Tagliaferro, P. A.; Brusco, A.; Uhl, G. R. *Brain Res.* **2006**, *1071*, 10. (c) Onaivi, E. S.; Ishiguro, H.; Gong, J.-P.; Patel, S.; Perchuk, A.; Meozzi, P. A.; Myers, L.; Mora, Z.; Tagliaferro, P.; Gardner, E.; Brusco, A.; Akinshola, B. E.; Liu, Q.-R.; Hope, B.; Iwasaki, S.; Arinami, T.; Teasenfitz, L.; Uhl, G. R. *Ann. N. Y. Acc. Sci.* **2006**, *1074*, 514. (d) Ellert-Miklaszewska, A.; Grajkowska, W.; Gabrusiewicz, K.; Kaminska, B.; Konarska, L. *Brain Res.* **2007**, *1137*, 161.
16. Rajesh, M.; Mukhopadhyay, P.; Hasko, G.; Huffman, J. W.; Mackie, K.; Pacher, P. *Br. J. Pharmacol.* **2008**, *153*, 347.
17. (a) Han, S.; Thatte, J.; Buzard, D. J.; Jones, R. M.; *J. Med. Chem.* **2013**, *56*, 8224. (b) Tabrizi, M. A.; Baraldi, P. G.; Borea, P. A.; Varani, K. *Chem. Rev.* **2016**, *116*, 519.
18. (a) Murineddu, G.; Asproni, B.; Pinna, G. A. *Rec. Pat. CNS Drug Discovery*, **2012**, *7*, 4. (b) Murineddu, G.; Deligia, F.; Dore, A.; Pinna, G.; Asproni, B.; Pinna, G. A. *Rec. Pat. CNS Drug Discovery*, **2013**, *8*, 42.
19. Malan Jr, T. P.; Ibrahim, M. M.; Lai, J.; Vanderah, T. W.; Makriyannis, A.; Porreca, F. *Curr. Opin. Pharmacol.* **2003**, *3*, 62.
20. Quartilho, A.; Mata, H. P.; Ibrahim, M. M.; Vanderah, T. W.; Porreca, F.; Makriyannis, A.; Malan Jr, T. P. *Anesthesiology*, **2003**, *99*, 955.
21. Hollinshead, S. P.; Tidwell, M. W.; Palmer, J.; Guidetti, R.; Sanderson, A.; Johnson, M. P.; Chambers, M. G.; Oskins, J.; Stratford, R.; Astles, P. C. *J. Med. Chem.* **2013**, *56*, 5722.
22. (a) Arevalo-Martin, A.; Vela, J. M.; Molina-Holgado, E.; Borrell, J.; Guaza, C. *J. Neurosci.* **2003**, *23*, 2511. (b) Zajicek, J. P.; Apostu, V. I. *CNS Drugs*, **2011**, *25*, 187. (c) Gijsen, H. J.-M.; De Cleyn, M. A.-J.; Surkyn, M.; Van Lommen, G. R.-E.; Verbist, B. M.-P.; Nijssen, M. J. M.-A.; Meert, T.; Van Wauwe, J.; Aerssens, J.; *Bioorg. Med. Chem. Lett.* **2012**, *22*, 547. (d) Han, S.; Zhang, F.-F.; Qian, H.-Y.; Chen, L.-L.; Pu, J.-B.; Xie, X.; Chen, J.-Z. *J. Med. Chem.* **2015**, *58*, 5751.
23. (a) Aso, E.; Juvés, S.; Maldonado, R.; Ferrer, I. *J. Alzheimer Dis.* **2013**, *35*, 847. (b) Aso, E.; Ferrer, I. *Frontiers in Pharmacology*, **2014**, *5*, 1. (c) Cao, C.; Li, Y.; Liu, H.; Bai, G.; Mayl, J.; Lin, X.; Sutherland, K.; Nabar, N.; Cai, J. *J. Alzheimer Dis.* **2014**, *42*, 973.
24. Kim, K.; Moore, D. H.; Makriyannis, A.; Abood, M. E. *Eur. J. of Pharmacol.* **2006**, *542*, 100.
25. Lunn, C. A.; Reich, E.-P.; Fine, J. S.; Lavey, B.; Kozlowski, J. A.; Hipkin, R. W.; Lundell, D. J.; Bober, L. *Br. J. Pharmacol.* **2008**, *153*, 226.
26. (a) Yang, P.; Myint, K.-Z.; Tong, Q.; Feng, R.; Cao, H.; Almehizia, A. A.; Alqarni, M. H.; Wang, L.; Bartlow, P.; Gao, Y.; Gertsch, J.; Teramachi, J.; Kurihara, N.; Roodman, G. D.; Cheng, T.; Xie, X.-

- Q. *J. Med. Chem.* **2012**, *55*, 9973. (b) Yang, P.; Wang, L.; Feng, R.; Almezhizia, A. A.; Tong, Q.; Myint, K.-Z.; Ouyang, Q.; Alqarni, M. H.; Wang, L.; Xie, X.-Q. *J. Med. Chem.* **2013**, *56*, 2045.
27. (a) Feng, Z.; Alqarni, M. H.; Yang, P.; Tong, Q.; Chowdhury, A.; Wang, L.; Xie, X.-Q. *J. Chem. Inf. Model.* **2014**, *54*, 2483. (b) Bertini, S.; Parkkari, T.; Savinainen, J. R.; Arena, C.; Saccomanni, G.; Saguto, S.; Ligresti, A.; Allarà, M.; Bruno, A.; Marinelli, L.; Di Marzo, V.; Novellino, E.; Manera, C.; Macchia, M.; *Eur. J. Med. Chem.* **2015**, *90*, 526. (c) Bertini, Chicca, A.; Arena, C.; Chicca, S.; Saccomanni, G.; Gertsch, J.; Manera, C.; Macchia, M.; *Eur. J. Med. Chem.* **2016**, *116*, 252. (d) Hu, J.; Feng, Z.; Ma, S.; Zhang, Y.; Tong, Q.; Alqarni, M. H.; Gou, X.; Xie, X.-Q. *J. Chem. Inf. Model.* **2016**, *56*, 1152.
28. (a) Rinaldi-Carmona, M.; Barth, F.; Millan, J.; Derocq, J.-M.; Casellas, P.; Congy, C.; Oustric, D.; Sarran, M.; Bouaboula, M.; Calandra, B.; Portier, M.; Shire, D.; Brelière, J.-C.; Le Fur, G. *J. Pharmacol. Exp. Ther.* **1998**, *284*, 644. (b) Portier, M.; Rinaldi-Carmona, M.; Pecceu, F.; Combes, T.; Poinot-Chazel, C.; Calandra, B.; Barth, F.; Le Fur, G.; Casellas, P. *J. Pharmacol. Exp. Ther.* **1999**, *288*, 582.
29. Mussinu, J.-M.; Ruiu, S.; Mule, A. C.; Pau, A.; Carai, M. A. M.; Loriga, G.; Murineddu, G.; Pinna, G. A. *Bioorg. Med. Chem.* **2003**, *11*, 251.
30. (a) Chen, J.-Z.; Wang, J.; Xie, X.-Q. *J. Chem. Inf. Model.* **2007**, *47*, 1626. (b) Kotsikorou, E.; Navas III, F.; Roche, M. J.; Gilliam, A. F.; Thomas, B. F.; Seltzman, H. H.; Kumar, P.; Song, Z.-H.; Hurst, D. P.; Lynch, D. L.; Reggio, P. H. *J. Med. Chem.* **2013**, *56*, 6593.
31. Pinna, G.; Curzu, M. M.; Dore, A.; Lazzari, P.; Ruiu, S.; Pau, A.; Murineddu, G.; Pinna, G. A. *Eur. J. Med. Chem.* **2014**, *85*, 747.
32. Pinna, G.; Loriga, G.; Lazzari, P.; Ruiu, S.; Falzoi M.; Frau, S.; Pau, A.; Murineddu, G.; Asproni, B.; Pinna, G. A. *Eur. J. Med. Chem.* **2014**, *82*, 281.
33. Dore, A.; Asproni, B.; Scampuddu, A.; Pinna, G. A.; Christoffersen, C. T.; Langgård, M.; Kehler, J. *Eur. J. Med. Chem.* **2014**, *84*, 181.
34. Cheng, Y.; Prusoff, W. H. *Biochem. Pharmacol.* **1973**, *22*, 3099.
35. Tabrizi, M. A.; Baraldi, P. G.; Ruggiero, E.; Saponaro, G.; Baraldi, S.; Poli, G.; Tuccinardi, T.; Ravani, A.; Vincenzi, F.; Borea, P. A.; Varani, K. *Eur. J. Med. Chem.* **2016**, *113*, 11.
36. Bolognini, D.; Cascio, M. G.; Parolaro, D.; Pertwee, R. G. *Br. J. Pharmacol.* **2012**, *165*, 2561.
37. Kenakin, T. *FASEB J.* **2001**, *15*, 598.
38. Cichero, E.; Menozzi, G.; Guariento, S.; Fossa, P. *Med. Chem. Commun.* **2015**, *6*, 1978.
39. Montero, C.; Campillo, N. E.; Goya, P.; Páez, J. A. *Eur. J. Med. Chem.* **2005**, *40*, 75.

40. Deiana, V.; Gómez-Cañas, M.; Pazos, M. R.; Fernández-Ruiz, J.; Asproni, B.; Cichero, E.; Fossa, P.; Muñoz, E.; Deligia, F.; Murineddu, G.; García-Arencibia, M.; Pinna, G. A. *Eur. J. Med. Chem.* **2016**, *112*, 66.
41. van de Waterbeemd, H.; Gifford, E. *Nat. Rev. Drug Discov.* **2003**, *2*, 192.
42. Suchocki, J. A.; May, E. L.; Martin, T. J.; George, C.; Martin, B. R. *J. Med. Chem.* **1991**, *34*, 1003.
43. Zhao, M.; Kuang, C.; Yang, Q.; Cheng, X. *Tetrahedron Letters* **2011**, *52*, 992
44. Verma, A. K.; Lotla, S. K. R.; Choudhary, D.; Patel, M.; Tiwari, R. K. *J. Org. Chem.* **2013**, *78*, 4386.
45. Merighi, S.; Simioni, C.; Gessi, S.; Varani, K.; Borea, P. A. *Biochem. Pharmacol.* **2010**, *79*, 471.
46. Bradford, M. M. *Anal. Biochem.* **1976**, *72*, 248.
47. Munson, P. J.; Rodbard, D. *Anal. Biochem.* **1980**, *107*, 220.
48. MOE: Chemical Computing Group Inc. Montreal. H3A 2R7 Canada. <http://www.chemcomp.com>
49. Gouldson, P.; Calandra, B.; Legoux, P.; Kernéis, A.; Rinaldi-Carmona, M.; Barth, F.; Le Fur, G.; Ferrara, P.; Shire, D. *Eur. J. Pharmacol.* **2000**, *28*, 17.
50. Sybyl-X 1.0 Tripos Inc 1699 South Hanley Road. St Louis. Missouri. 63144. USA 25.
51. (a) Fossa, P.; Cichero, E. *Bioorg. Med. Chem.* **2015**, *23*, 3215. (b) Franchini, S.; Battisti, U. M.; Prandi, A.; Tait, A.; Borsari, C.; Cichero, E.; Fossa, P.; Cilia, A.; Prezzavento, O.; Ronsisvalle, S.; Aricò, G.; Parenti, C.; Brasili, L. *Eur. J. Med. Chem.* **2016**, *112*, 1.

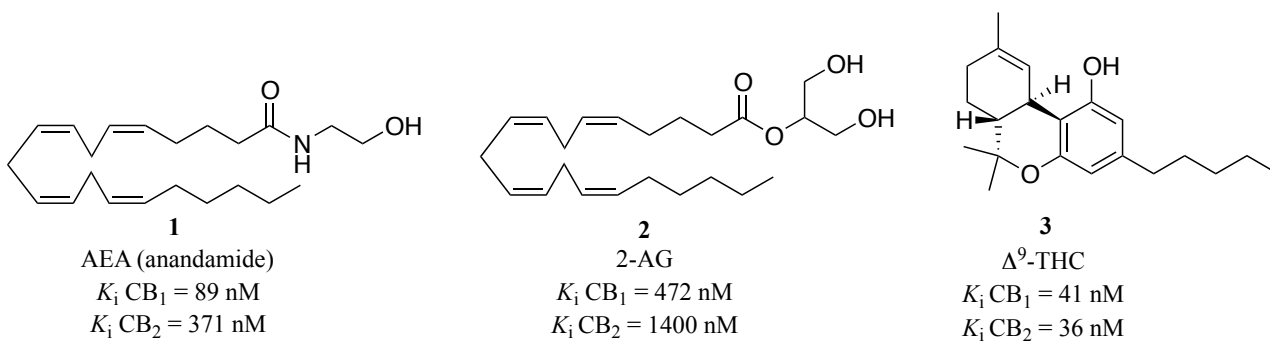
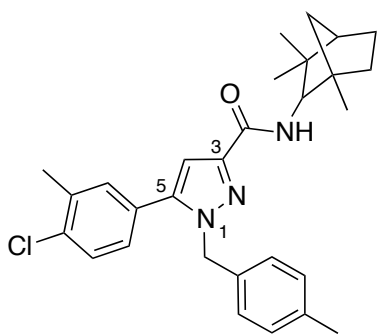


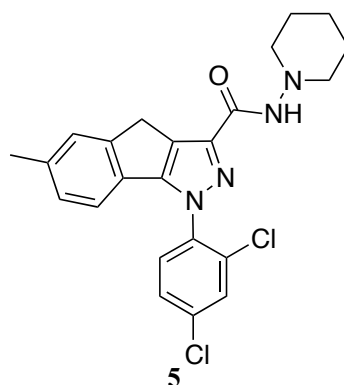
**Figure 1.** The major endogenous ligands and Δ<sup>9</sup>-THC for cannabinoid receptors.





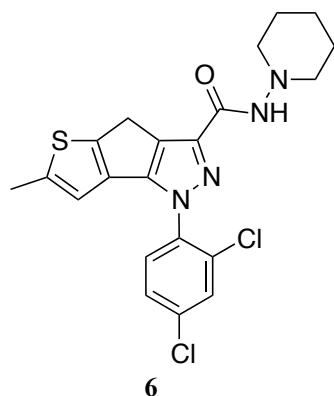
4 (SR144528)

$K_iCB_2 = 0.6 \text{ nM}$   
 $K_iCB_1 = 400 \text{ nM}$   
 selectivity ratio  $K_iCB_1/K_iCB_2 = 666:1$



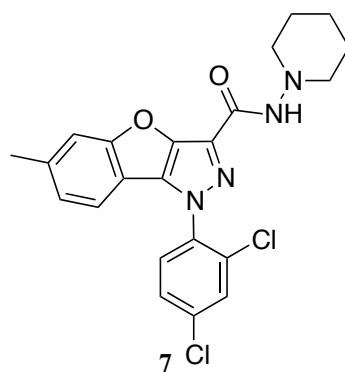
5

$K_iCB_2 = 0.037 \text{ nM}$   
 $K_iCB_1 = 363 \text{ nM}$   
 selectivity ratio  $K_iCB_1/K_iCB_2 = 9810:1$



6

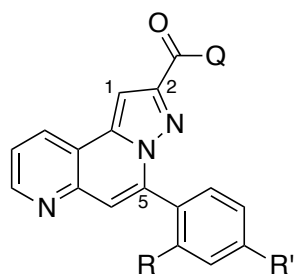
$K_iCB_2 = 2.3 \text{ nM}$   
 $K_iCB_1 = 440 \text{ nM}$   
 selectivity ratio  $K_iCB_1/K_iCB_2 = 191.3:1$



7

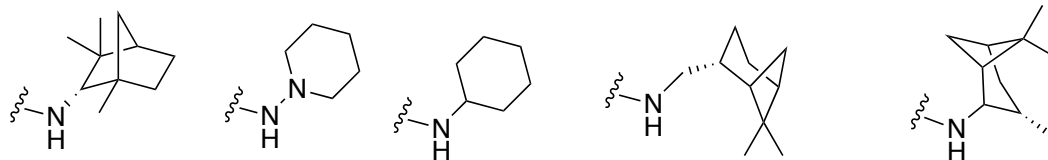
$K_iCB_2 = 12.9 \text{ nM}$   
 $K_iCB_1 = 1788 \text{ nM}$   
 selectivity ratio  $K_iCB_1/K_iCB_2 = 138.6:1$

**Figure 2.** Chemical structures of **CB<sub>2</sub>** selective ligands.

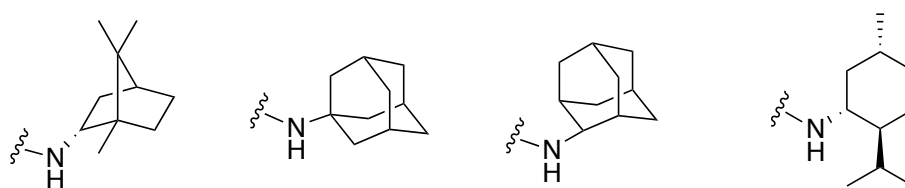


**8a-k**

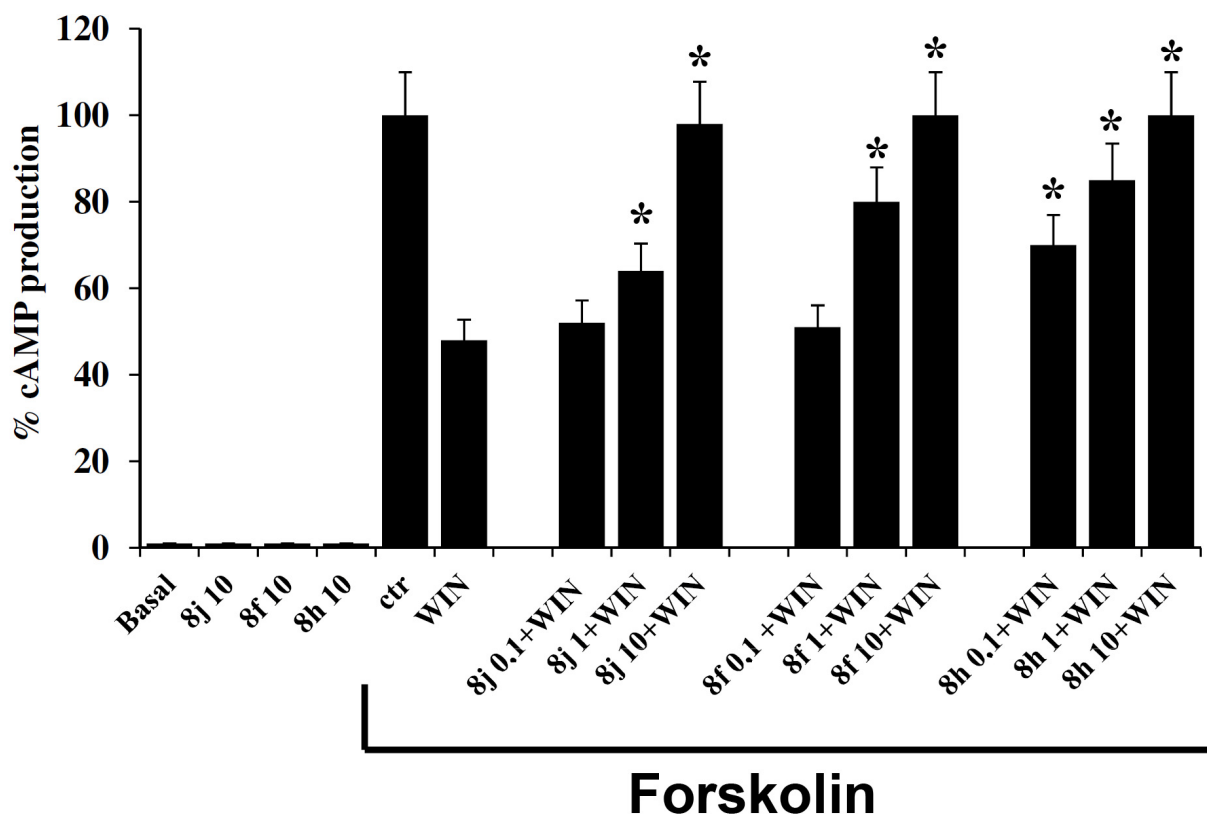
R: H, Cl; R': CH<sub>3</sub>, Cl



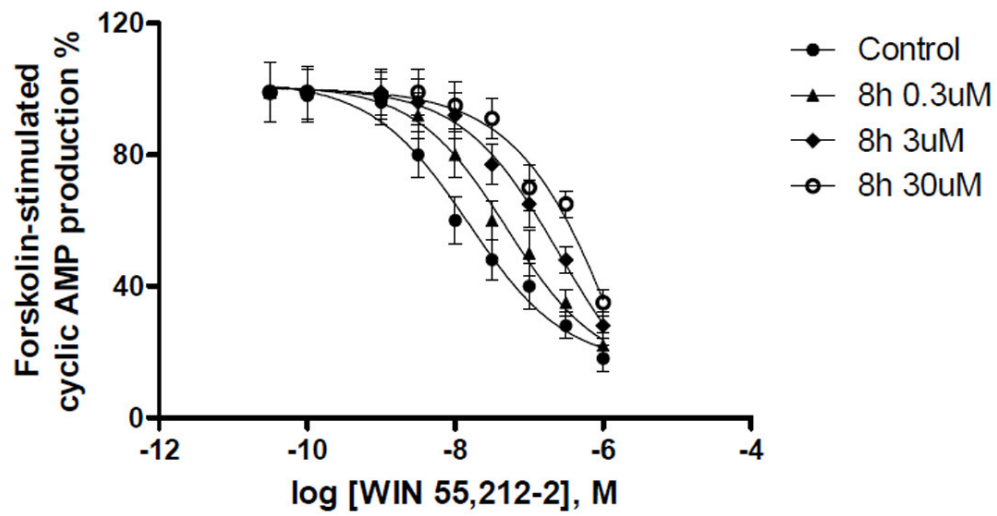
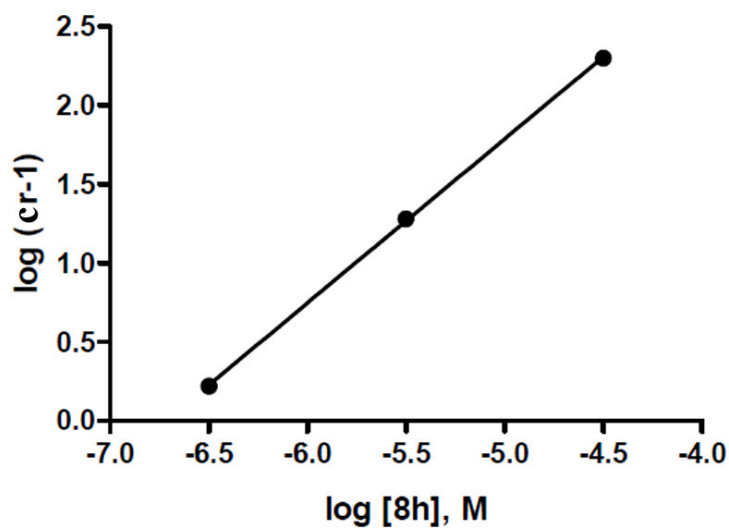
Q:



**Figure 3.** Novel 5-aryl-pyrazolo[5,1-*f*][1,6]naphthyridine-2-carboxamides **8a-k**.



**Figure 4.** Inhibition of forskolin-stimulated cAMP levels (100%) by WIN 55,212-2 (0.1  $\mu$ M) and antagonism by **8j**, **8f**, and **8h** (0.1-10  $\mu$ M) in hCB<sub>2</sub>CHO cells. Forskolin (10  $\mu$ M) effect was set to 100%. The effect of compounds alone **8j**, **8f**, and **8h** (10  $\mu$ M) is shown. Values are the mean $\pm$ SEM of four independent experiments (N=4). \*P<0.05, compared with WIN 55,212-2; analysis was by ANOVA followed by Dunnett's test.

**A****B**

**Figure 5.** A, concentration-response curves of WIN 55,212-2 in hCB<sub>2</sub>CHO cells in the absence and presence of various concentrations of **8h**. B, Schild plot of **8h** against WIN 55,212-2. Abscissa, log of the molar concentration of the antagonist **8h**. Ordinate, log of the concentration ratio -1 (cr - 1) of the agonist WIN 55,212-2. Values are the mean±SEM of four independent experiments (N=4).

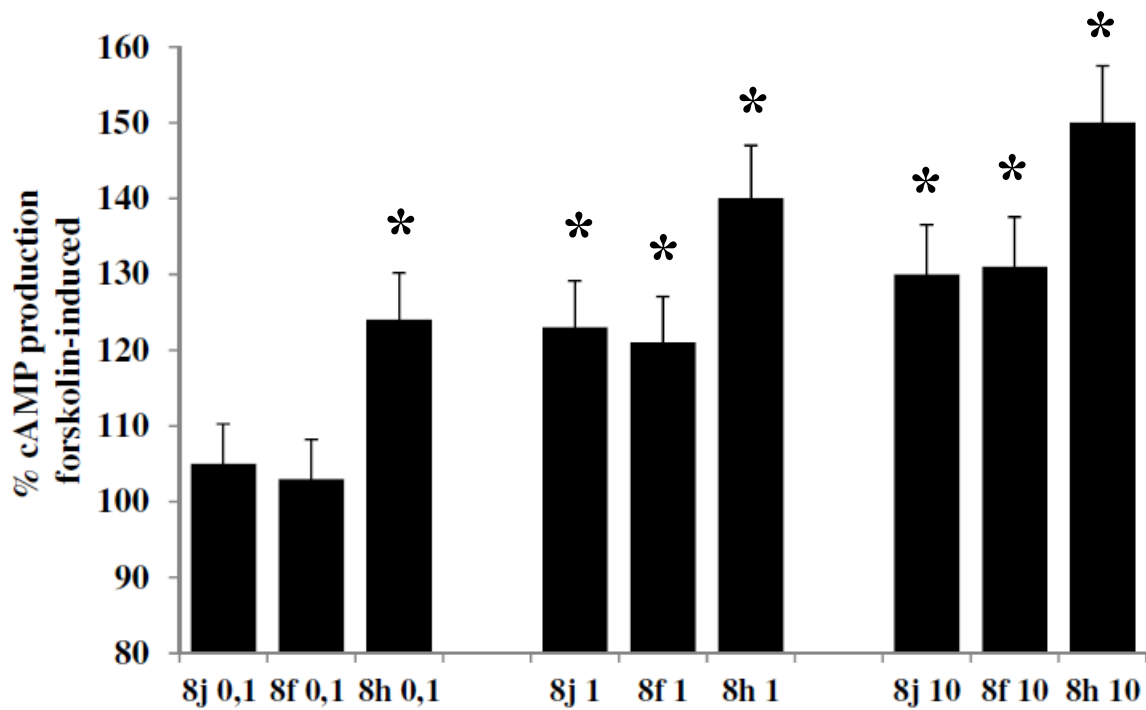


**Figure 6.** Effect of **8j**, **8f**, and **8h** (0.1-10 μM) expressed as % of increase of forskolin-stimulated cAMP accumulation (100%) in hCB<sub>2</sub>CHO cells. Forskolin (10 μM) effect was set to 100%. Values are the mean±SEM of four independent experiments (N=4). \*P<0.05, compared with Forskolin (10 μM); analysis was by ANOVA followed by Dunnett's test.

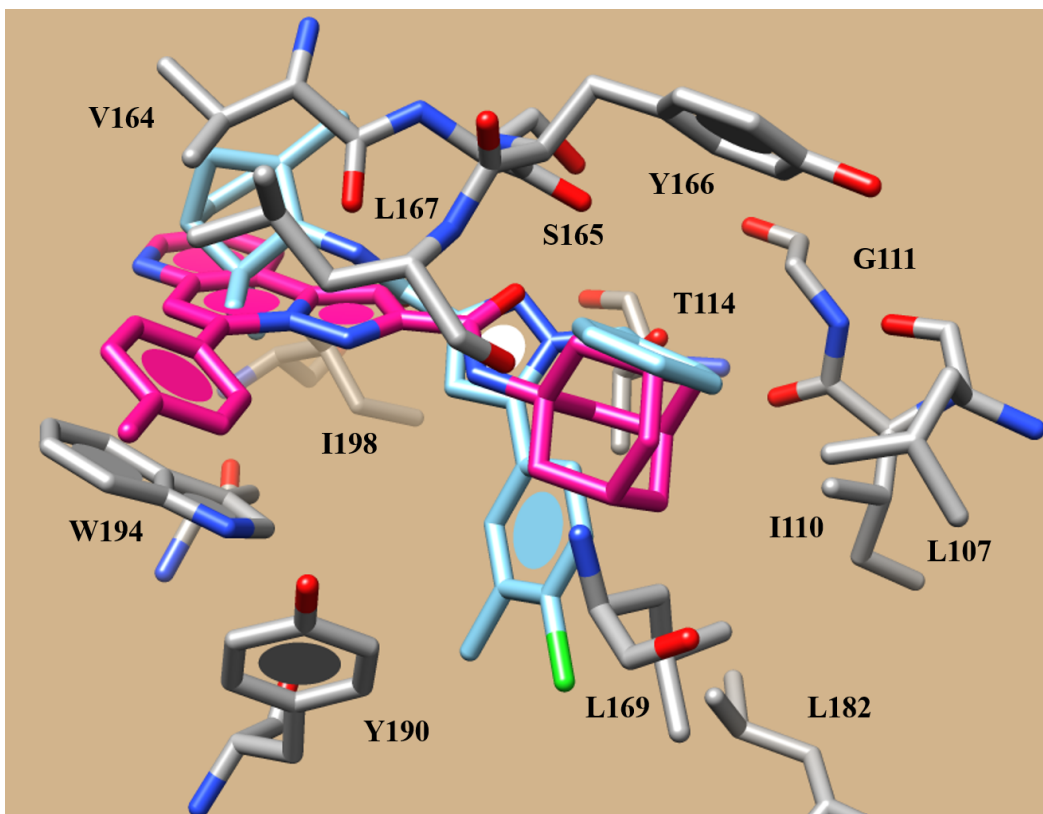


**Figure 7.** SR144528 (C atom: cyan) and compound **8h** (C atom: deep magenta) docking poses into the **hCB<sub>2</sub>** inverse agonist binding site. The most important residues are labelled.

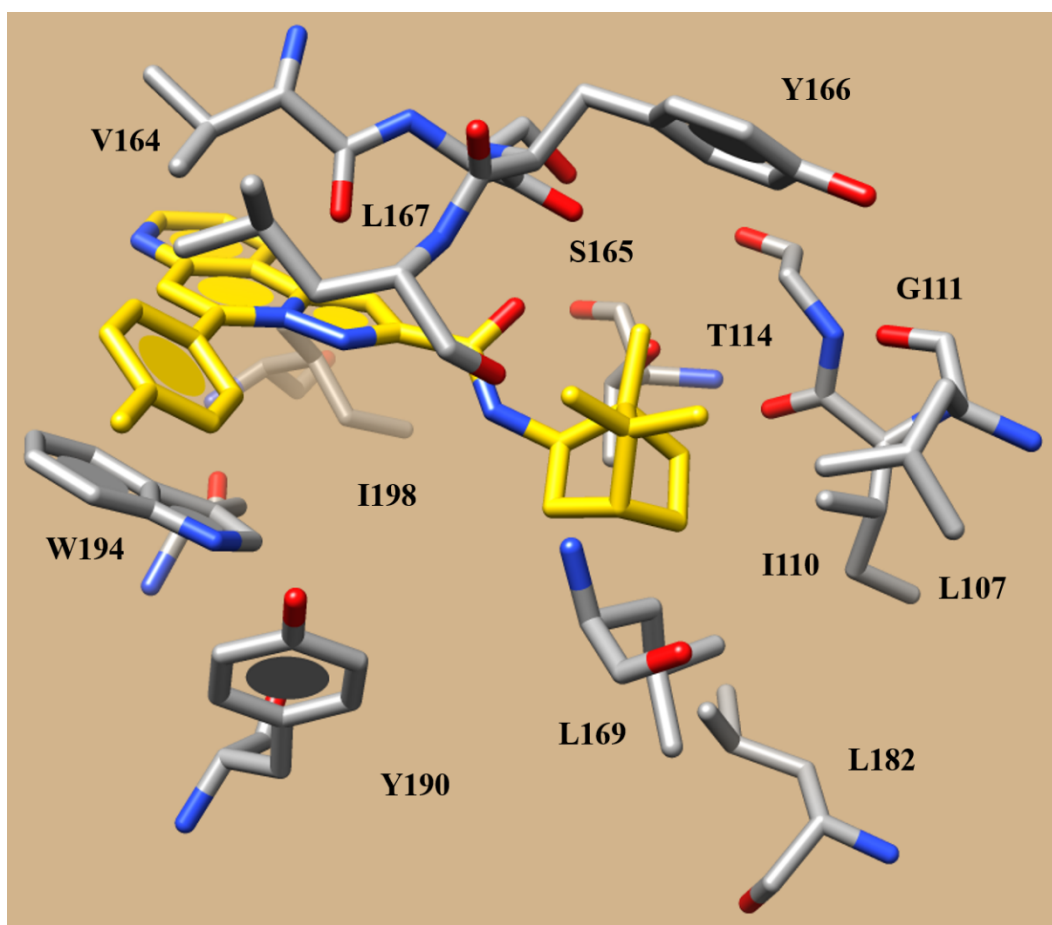


**Figure 8.** Docking poses of compound **8f** (C atom: yellow) within the *hCB<sub>2</sub>* inverse agonist binding site. The most important residues are labelled.

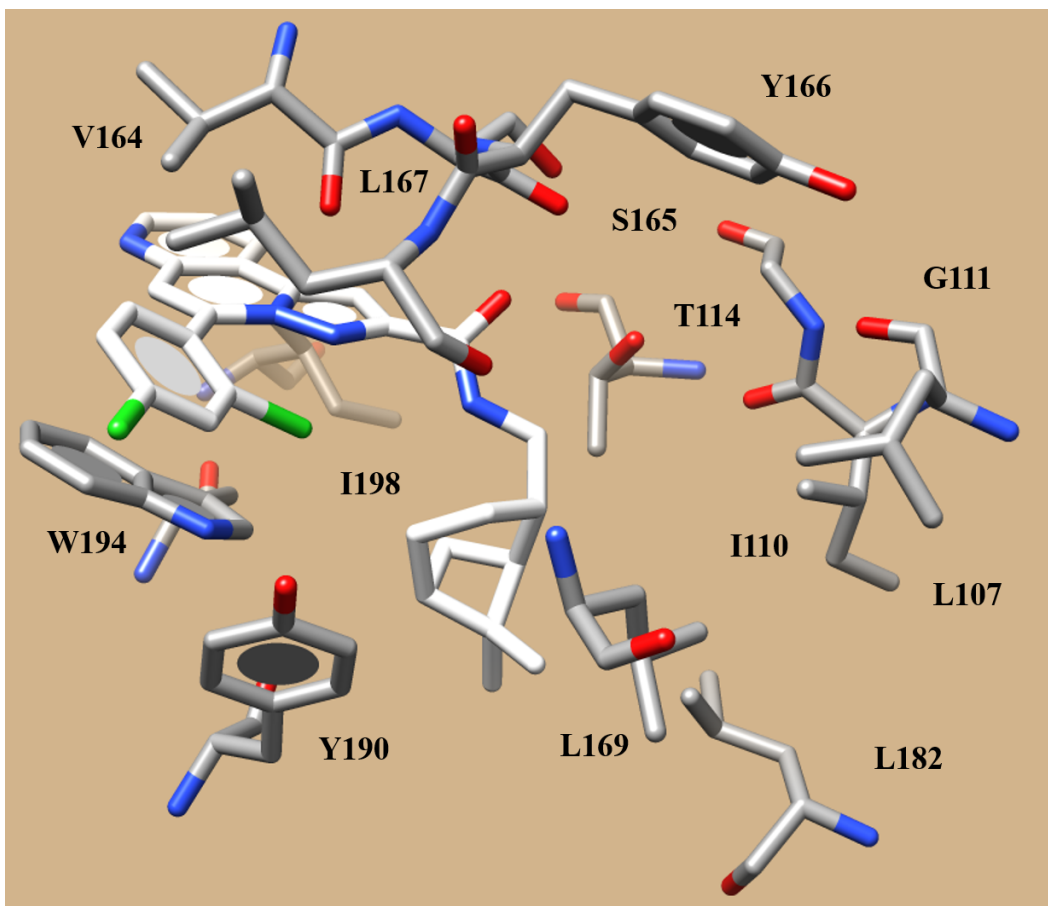
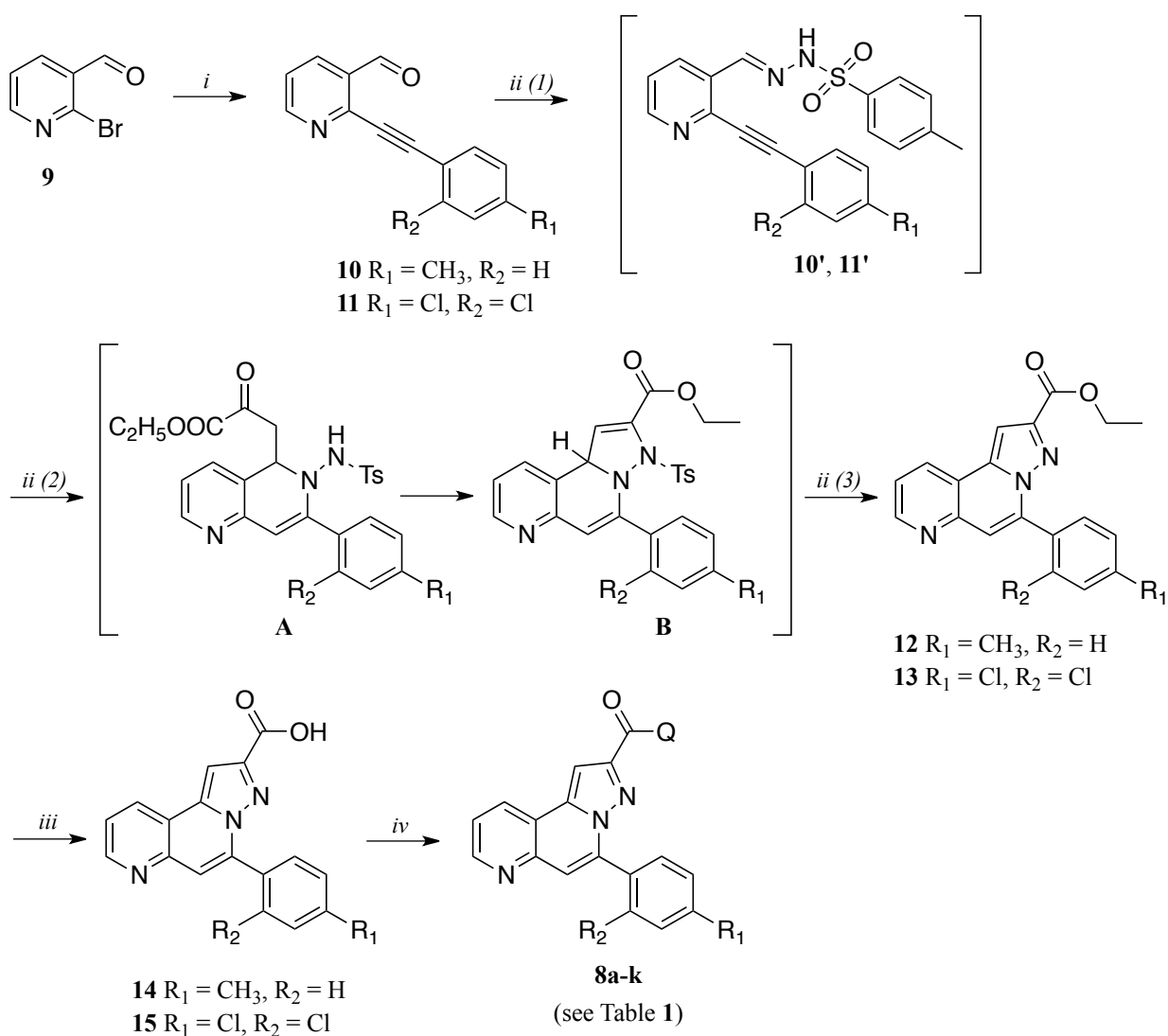


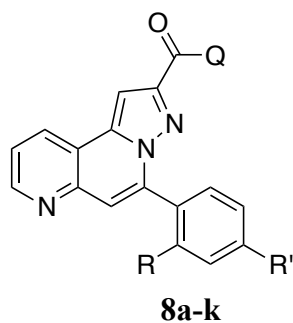
**Figure 9.** Docking poses of compound **8j** (C atom: white) within the *hCB<sub>2</sub>* inverse agonist binding site. The most important residues are labelled.





**Scheme 1.** Reagent and conditions: (i) *p*-tolylacetylene (for **10**) or 2,4-dichlorophenylacetylene (for **11**), Pd(PPh<sub>3</sub>)<sub>2</sub>Cl<sub>2</sub>, CuI, Et<sub>3</sub>N, dry DMF, MW 60 °C, 20 min; (ii) (1) PTSH, AgOTf, DL-proline, dry EtOH, r.t. 10 min. (2) Ethyl pyruvate, MW 60 °C, 3.5 h; (3) Na<sub>2</sub>CO<sub>3</sub>, r.t. 12 h; (iii) NaOH, THF, 40 °C, 3h; (iv) (1) pivaloyl chloride, Et<sub>3</sub>N, dry CH<sub>2</sub>Cl<sub>2</sub>, 0 °C to r.t., 2h; (2) amine, CH<sub>2</sub>Cl<sub>2</sub>, Et<sub>3</sub>N, 0 °C to r.t., 2.5 h.

**Table 1.** Structures and binding data<sup>a</sup> for compounds **8a-k** and **WIN 55,212-2**.



Compd	R	R'	Q	Receptor affinity (nM)		CB <sub>2</sub> selectivity
				K <sub>i</sub> CB <sub>1</sub>	K <sub>i</sub> CB <sub>2</sub>	K <sub>i</sub> CB <sub>1</sub> /K <sub>i</sub> CB <sub>2</sub>
<b>8a</b>	H	CH <sub>3</sub>		2200 ± 190	800 ± 84	2.7
<b>8b</b>	H	CH <sub>3</sub>		> 10000	> 1000	-
<b>8c</b>	H	CH <sub>3</sub>		> 10000	2133 ± 230	> 4.7
<b>8d</b>	H	CH <sub>3</sub>		> 10000	120 ± 15	> 83
<b>8e</b>	H	CH <sub>3</sub>		> 10000	240 ± 28	> 42
<b>8f</b>	H	CH <sub>3</sub>		7000 ± 680	53 ± 7	132
<b>8g</b>	H	CH <sub>3</sub>		3300 ± 270	280 ± 30	12
<b>8h</b>	H	CH <sub>3</sub>		5700 ± 550	33 ± 2	173
<b>8i</b>	H	CH <sub>3</sub>		> 10000	133 ± 15	> 75
<b>8j</b>	Cl	Cl		> 10000	67 ± 8	> 149
<b>8k</b>	Cl	Cl		ND <sup>b</sup>	ND	
<b>WIN 55,212-2</b>				13 ± 2	2.5 ± 0.3	5.2

<sup>a</sup> Affinity of compounds to CB<sub>1</sub>R and CB<sub>2</sub>R was assayed using transfected human CB<sub>1</sub> and CB<sub>2</sub> CHO cells and [<sup>3</sup>H]CP-55,940 as radiolabeled ligand. K<sub>i</sub> values are the mean ± SEM of at least three independent experiments run in triplicate.

<sup>b</sup> ND, not determined.

**Table 2.** Calculated ADMET descriptors related to absorption and distribution properties.

<b>Compd</b>	<b>cLogP</b>	<b>LogBB<sup>a</sup></b>	<b>LogPS<sup>b</sup></b>	<b>HIA (%)<sup>c</sup></b>	<b>Vd (l/kg)<sup>d</sup></b>	<b>%PPB</b>	<b>LogKa<sup>HSA</sup></b>	<b>%F (oral)</b>
<b>8f</b>	5.00	0.44	-1.1	100	2.7	97.92	4.68	97.3
<b>8h</b>	4.89	0.27	-1.1	100	2.7	98.26	4.94	78.6
<b>8j</b>	6.12	0.00	-1.3	100	3.6	99.00	5.47	34.6
<b>SR144528 (4)</b>	6.19	0.37	-1.3	100	4.0	98.96	5.39	89.0

<sup>a</sup> Extent of brain penetration based on ratio of total drug concentrations in tissue and plasma at steady-state conditions; <sup>b</sup> Rate of passive diffusion-permeability. PSA represents Permeability-Surface area product and is derived from the kinetic equation of capillary transport; <sup>c</sup> HIA represents the human intestinal absorption, expressed as percentage of the molecule able to pass through the intestinal membrane; <sup>d</sup> Prediction of Volume of distribution (Vd) of the compound in the body.

**Table 3.** Calculated ADMET descriptors related to metabolism, excretion and toxicity properties.

Compd	P-glycoprotein substrate (R.I. $\geq$ 0.40)	CYP3A4		LD <sub>50</sub> (mg/kg) <sup>a</sup> (R.I. $\geq$ 0.40 )
		Inhibitor (IC <sub>50</sub> < 10 $\mu$ M) (R.I. $\geq$ 0.40)	Substrate (R.I. $\geq$ 0.40)	
8f	not	0.50	0.99	430
8h	not	0.32	0.98	320
8j	not	0.21	0.98	270
SR144528 (4)	not	0.39	0.99	440

<sup>a</sup> Acute toxicity (LD<sub>50</sub>) for mouse after oral administration (RI: reliability index. Borderline-allowed values for reliability parameter are  $\geq$  0.3, the most predictive fall in the range 0.50-1.0).